Universiteit Utrecht

Faculty of Geoscience

Tracing organic carbon through the Godavari River basin (India) using plant waxes and stable isotopes

Paulina Concha Hernández

Master Thesis

First supervisor: Frédérique Kirkels MSc.

Second supervisor: dr. ir. Francien Peterse

August 2017

Abstract

Plant waxes help to protect plants against moisture loss. These waxes consist of *n*-alkanes which are resistant against degradation and can persist in different environments. The chain length and carbon isotopic compositions of *n*-alkanes are characteristics of different vegetation types, and can thus be used to reconstruct past climate conditions when analysed in a sedimentary archive. However, the interpretation of plant wax records in coastal sediments cannot always be directly linked to processes observed in the modern system, i.e. what is observed in plants, soils and sediments in the adjacent river catchment. In this study the *n*-alkanes and isotopes of bulk organic carbon in the monsoon-influenced Godavari river basin, India are determined to trace the transport of vegetation-derived organic carbon throughout the catchment until discharge to the Bay of Bengal.

The river basin is characterised by a precipitation gradient, which influenced its vegetation. The upper area of the catchment receives little precipitation and the contribution of C4 plants is relatively larger compared to the lower area of the basin, where there is more precipitation. Indeed, in the upper catchment, soils are enriched in ^{13}C, while in the lower catchment their signals are more depleted. Vegetation patterns in the upper catchment indicate that C3 species affected by moisture stress contribute to enriched signatures found in the soils.

Differences between wet and dry seasons indicate that organic carbon from the lower catchments is discharged by the Godavari river mainly during wet season, trend that is supported by *n*-alkanes distributions in the delta.

Table of Contents

Table of Figures

List of tables

1. Introduction

Leaf cuticles from plants are composed of a layer of wax which protects them from mechanical damage, predation, and moisture loss (Eglinton and Hamilton, 1967). The main constituents of this wax are *n*-alkanes, which are characterized by their strong bonds between hydrocarbons and the lack of functional groups. These properties permit *n*-alkanes to resist degradation making them an excellent biomarker (Eglinton and Eglinton, 2008).

Certain characteristics of the hydrocarbon chains have been linked to different types of plants, climates, and environments (Meyers & Ishiwatari, 1993; Bush & McInerney, 2013; Carr et al., 2014; Eglinton and Eglinton, 2008). For instance, leaf wax *n*-alkanes, commonly have long chain lengths with odd carbon-numbered members predominating over the even carbon-numbered members (Eglinton & Hamilton, 1967). Long-chain *n*-alkanes are main components vascular plants (Eglinton & Hamilton, 1967), characterized by shorter chain lengths between C3 plants and longer homologues in C4 plants (Meyers & Ishiwatari, 1993; Meyers, 2003). While, in a smaller range, short-chain *n*-alkanes between *n*-C_{17} and *n*-C_{21} are dominant in aquatic algae (Giger et al., 1980; Cranwell et al., 1987; Castañeda & Schouten, 2011). One way to characterised *n*-alkane distributions is by calculating their average chain length (ACL) (Bush & McInerney, 2013). This index has served as an indicator of changes in vegetation, linked to variations in temperature or aridity (Rommerskirchen et al., 2003; Castañeda & Schouten, 2011). In addition to ACL, ratios of individual *n*-alkane abundances have also been used to characterise, for instance, the contribution of aquatic algae (Paq) (Ficken et al., 2000).

Moreover, isotopic fractionation in environmental processes can complement the study of leaf wax *n*-alkanes. When comparing carbon isotope ratios, $\delta^{13}C$ values can be used as indicative of C3 and C4 plants (Eglinton and Eglinton, 2008; Castañeda & Schouten, 2011). The plant types vary in the pathway they use to fix CO_2 for photosynthesis. The C3 pathway begins with the diffusion of CO_2 from the atmosphere into the air-filled spaces within the leaf i.e. stomatal pores. Diffusion and discrimination of ^{13}C by rubisco enzyme leads to depleted values compared to atmospheric CO_2. In C4 plants, discrimination by PEP enzyme and subsequently catabolism of CO_2 leads to less depleted $\delta^{13}C$ values compared to the C3 pathway (Marshall et al., 2007). Isotopic signatures have been largely studied and distinguished between plants, with ranges between −20‰ and −34‰ for C3 plants and the most frequent values around −27‰. Whereas C4 plants range between −9‰ and −19‰, with the most frequent values around −13‰ (Rao et al., 2017, Deines,

1980; O'Leary, 1981, 1988; Farquhar et al., 1989; Sage et al., 1998). Other studies have focused on the hydrogen isotopic composition of plant waxes, i.e. δD. The primary driver of the hydrogen isotopic composition of plant waxes is the composition of the precipitation the plant receives, which is used to synthesize the waxes. Therefore, the occurrence, distribution, and isotopic composition of *n*-alkanes in sedimentary archives have been widely used to correlate paleoecology and paleoclimatology processes (Kahmen et al., 2013; Sachse et al., 2006; Freeman & Colarusso, 2001).

However, the properties of plant waxes of modern vegetation and those in a sedimentary archive do not always match, suggesting that plant waxes are altered during transport from the plant to a sedimentary archive. This can, for example, be caused due to degradation processes or temporary storage during transport.

One way to clarify *n*-alkanes signature differences between plants and sedimentary records is to evaluate which factors are controlling leaf wax *n*-alkane distributions in a modern system, such as differences in leaf wax production between plant species, or the influence of (limiting) water availability. Secondly, it is key to understand how plant wax signatures are affected during transportation to a sedimentary archive. In the case of river fan sediments, this would require evaluating their distribution and carbon isotopic signatures from plants into the soil, entering a river as suspended particulate material, and finally sediments. In addition, *n*-alkanes can be used as a tracer for plant-derived organic carbon in fluvially transported organic carbon from land to sea.

1.1. Objectives

The broader aim of this research project will be to evaluate how the *n*-alkane signature that is discharged to the ocean to be stored in a coastal marine sedimentary record reflects the vegetation in the adjacent river catchment, and how this vegetation signature evolves during transit through a monsoon-driven river basin. Specifically, the objectives of this research will be to:

- Identify the distribution of *n*-alkanes in plants, soils, and river sediments in the Godavari River basin;
- Evaluate the distribution of $\delta^{13}C$ values of bulk organic carbon in plants, soils, suspended particulate matter (SPM) and river sediments.

The combination of vegetation patterns and climate variability, i.e. wet (monsoon) and dry seasons observed in the Godavari river basin (India), offers the opportunity to define end-members in carbon isotopic signatures for the different parts of the catchment and/or to determine the provenance of the material that is discharged to the ocean during dry and wet conditions. Thus, it makes this area very suitable to study any evolving differences between *n*-alkanes in plants, soils, suspended particulate matter, and sediments, as well as the effect of transport.

2. Study site

The Godavari river basin (Fig. 1) is the largest among the non-Himalayan rivers in India (Biksham & Subramanian, 1988a). The river has its source close to Nashik, in the Western Gaths, at an elevation of 920 m. This location is about 80 km east of the west coast of India, and from there, the river travels 1465 km in a south-east direction, discharging into the Bay of Bengal. The total catchment area is 313,147 km^2, of which 60% is occupied by the tributaries Purna, Pranhita, Indravati and Sabri located in the east part of the catchment area (Pradhan et al., 2014). In the delta, river discharge takes place through three distributaries, the Goutami, Vainateyam and Vasishta.

The main geological formations found in the river basin includes the Tertiary Deccan traps (48%) at the upstream end, Archean granites (39%) in the Indravati, Sabari and east-Pranhita sub-catchments (i.e. Eastern Ghats), and Precambrian and Gondwana sedimentary rocks (11%) in the lower part of the basin (Biksham & Subramanian, 1988b; Pradhan et al., 2014).

Semi-arid to monsoonal climate governs the catchment area. Annual average maximum temperature is about 33°C and the minimum is 24°C. Nevertheless, temperatures can reach a minimum of 17°C in December and maximum of 45°C in May (Rao et al., 2015). Annual rainfall is 1085 mm (Panda et al., 2011), from which 84% of the total occurs during South West Monsoon period, reaching maximum precipitation levels between July and September. During this period and extending until October, the river discharges 93.6% of the total annual flow (Rao et al., 2015). Between November and January, the river receives the remaining total annual rainfall (Pradhan et al., 2014).

The modern natural vegetation is a combination of savanna and tropical grassland present in the west area of the catchment, and tropical forest in the east of the catchment (Asouti & Fuller, 2008; Ponton et al., 2012). Main anthropogenic activities in the basin include agricultural practices, fertilizer, cement and paper industries and mining (Gupta et al., 1997).

Based on the configuration of the tributaries, six main regions can be distinguished in the Godavari river basin: Upper Godavari, Pranhita, Indravati, Middle Godavari, Dowleiswaram Reservoir and Delta (Fig. 1). The Upper Godavari region starts from the source of the Godavari river until the confluence with the Pranhita river. The Pranhita region consists of the Wardha, Wainganga and Pranhita basins. The Indravati regions comprise the catchment of the two large tributaries; the Indravati and the Sabari. The

Middle region covers the area where the Godavari river meets the Pranhita and Indravati rivers. The Dowleiswaram reservoir is the region that includes the Godavari river after all main tributaries converged until it meets the Dowleiswaram dam. The Delta includes the area after the dam and the three main distributaries. The whole catchment and a transect in the Delta region was sampled in high resolution as indicated in Fig. 1. Table 1 gives the sampling site labels from Fig 1. that were renamed during the second sampling campaign.

Table 1. Sampling location labels from Fig. 1 with their original identification.

Original ID	**Sampling location label**	**Original ID**	**Sampling location label**	**Original ID**	**Sampling location label**
ETH1	ETH1	G25	W25	G46	W46
ETH2	W52	G26	W26	G47	W47
ETH3	ETH3	G27	G27	G48	W48
ETH4	ETH4	G28	G28	LW1	LW1
ETH5	ETH5	G29	W29	LW2	LW2
ETH6	W53	G30	W30	LW3	LW3
ETH7	W51	G31	W31	Soil pit	Soil pit
ETH8	ETH8	G32	W32	T1	TW1
ETH9	ETH9	G33	W33	T2	TW2
G10	G10	G34	W34	T3	TW3
G14	G14	G35	G35	T4	TW4
G15	W15	G36	G36	T5	TW5
G16	W16	G37	W37	T6	TW6
G17	W17	G38	W38	W28	W28
G18	W18	G39	W39	W41	W41
G19	W19	G40	W40	X41	X41
G20	W20	G41	G41	X44	W49
G21	W21	G42	W42	X45	W50
G22	G22	G43	W43	X46	X46
G23	W23	G44	W44	X47	X47
G24	W24	G45	G45	X48	X48

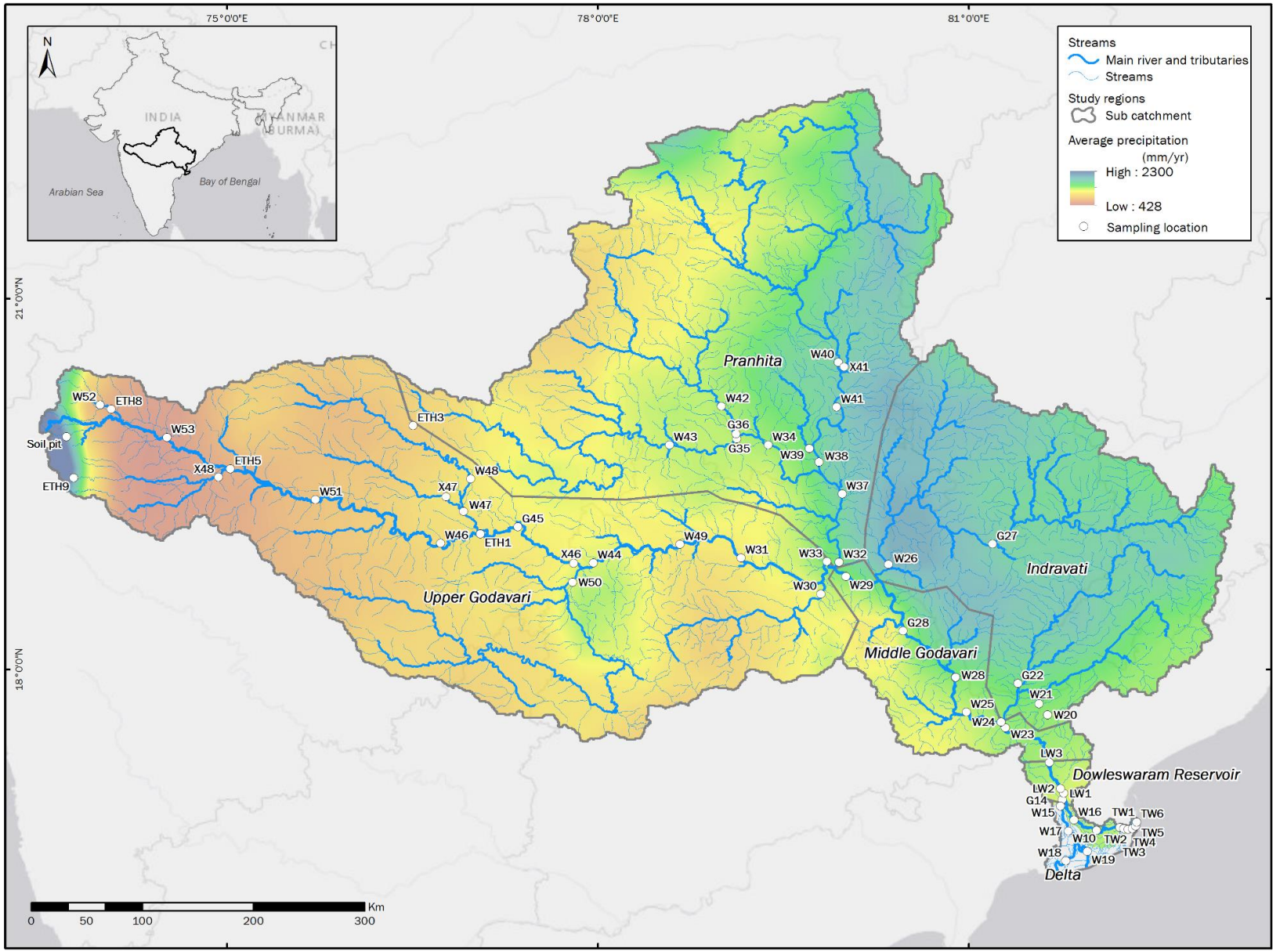

Figure 1. Location map of the study area with sampling sites through the Godavari river basin.

3. Materials and methods

3.1. Sample collection and preparation

Plant, surface soil, surface sediment and river water was collected at the locations shown in Figure 1. Soils and plants were collected during dry season conditions i.e. February-March 2015. Sediment and surface water were collected during wet season conditions i.e. July-August, 2015. The river water was filtered using pre-combusted 0.7µm GFF filters to obtain suspended particulate matter (SPM).

All samples were freeze-dried and homogenized, after which lipids were extracted using Accelerated Solvent Extraction (Thermo Scientific Dionex ASE 350). The obtained total lipid extract (TLE) was split into different fractions. For the river sediments, non-polar fractions, containing *n*-alkanes, were obtained by eluting 80% of the TLE over an activated aluminium oxide column, while *n*-alkane fractions for the soil and SPM samples were obtained after saponification of the TLEs. Vegetation data was derived from Martes, 2016.

3.2. Urea adduction

Non-polar fractions were cleaned using the urea adduction technique. This method is recommended for samples with an unresolved complex mixture (UCM) in their gas chromatograms. In general, UCM can contain alkanes, branched alkanes, cycloalkanes, monoaromatics, multi-ring aromatics, heteroatomic aromatics, among others (Frysinger et al., 2003). Urea forms crystalline inclusion compounds with straight chain compounds, excluding common hydrocarbons found in UCM (Nwadinigwe & Nwobodo, 1994).

The urea adduction protocol (Appendix A1) was adapted from JoVE Science Education Database (2017).

3.2.1. Urea adduction method

A solution of urea in methanol (1.5 mL) was added to the non-polar fraction which was dissolved in 1.5 mL of DCM:*n*-hexane (2:1) mixture. The mix was frozen for 30 minutes to complete the formation of urea adducts. The crystals were dried under a N_2 stream and then rinsed with *n*-hexane to obtain the non-adduct hydrocarbons. After the dissolution of the crystals, adducted *n*-alkanes were recovered with *n*-hexane.

3.2.2. Urea adduction test

Internal laboratory soil and sediments samples were tested to determine the recovery of *n*-alkanes after the urea adduction method. The method was optimised for freezing time,

rinsing procedure and tested at various concentrations; blanks were checked potential contamination. Each sample was tested with 3 consecutive urea adductions, analysing the *n*-alkane distribution and concentration after each adduction and calculating the recovery between each adduction and the total recovery (the last adduction compared to the untreated sample). Finally, the optimised procedure was applied on a sediment sample taken from the Godavari river to assess the applicability of the method on our samples.

3.3. *n*-alkanes analysis

A selection of soil, sediment and SPM fractions was treated with urea and analysed using Gas Chromatography (GC) to determine concentrations and distributions of long chain *n*-alkanes. GC was performed with a Hewlett-Packard 6893 Series instrument fitted with a capillary column (30 m x 320 µm i.d.) coated with CP Sil-5CB phase (0.10 µm film thickness) and a flame ionization detector (FID). Fractions were injected manually at 70°C and eluted using He as carrier gas; the temperature programme was: 70°C to 130°C at 20°C min^{-1}, 130–320°C at 4°C min^{-1}, holding 320°C for 20 minutes. The *n*-alkanes were identified by their retention time in comparison with *n*-alkanes from a commercial alkane standard, containing even *n*-alkanes (*n*-C_{10} – *n*-C_{40}). Depending on the peak heights, samples containing enough *n*-alkanes were integrated using Agilent GC Chemstation software (Rev. P.04.03DSP1). The *n*-alkanes were quantified comparing peak areas to a co-injected squalane standard.

3.4. Isotopic analysis

3.4.1. Bulk $\delta^{13}C$ composition

Soils and SPM samples were decalcified using vapour acidification (Komada et al., 2008; Van der Voort et al., 2016). GF/F filters containing SPM and soil samples were put in pre-combusted Ag capsules (15x8x8 mm, Elemental Microanalysis, Okehampton, United Kingdom) and placed in a desiccator at 70°C with 37% HCl for 72h and subsequently dried for a minimum of 120h with NaOH at 70°C. Soil, SPM and plant samples were analysed to determine bulk organic carbon and carbon isotopic composition using a Flash 2000 Organic Element Analyser (EA) fitted with a MAS 200 Autosampler coupled via a Thermo ConfloIV to Thermo Delta V Advantage Isotope Ration MS (IRMS) at the Royal NIOZ. Integration was performed through ISODAT 3.0 software. Delta values were corrected using acetanilide as internal standard and corroborated with casein and urea standards.

3.4.2. *n*-alkanes $\delta^{13}C$ composition

A selection of alkane fractions analysed in GC were also analysed using a Gas Chromatographer coupled to an Isotope Ratio Mass Spectrometry (GC-IRMS) to determine the compound-specific $\delta^{13}C$ of *n*-alkanes. Carbon isotope analysis was performed using Agilent 6890 Gas Chromatographer coupled to a Thermo Finnigan Trace DELTAplus XP Isotope Ratio Mass Spectrometer using a CP-Sil 5 column (25 m x 320 µm i.d.). Helium was used as a carrier gas with a constant flow of 1 ml/min and the oven heated 20°C min^{-1} from 70°C to 130°C, continuing with 4°C min^{-1} to 280°C, temperature that was held for 20 minutes. Before samples were analysed in duplicate, isotopic ratios were calibrated using the reference standard Schimmelmann B (purchased from A. Schimmelmann, Biogeochemical Laboratories, Indiana University). Identification of peaks was possible by comparing retention times with co-injected squalane standard. Integration and calculation of $\delta^{13}C$ was performed through ISODAT NT (version 2.0) software.

3.5. Data processing

3.5.1. Indices and statistics

Average chain length (ACL) was calculated using the concentration of odd and even chain lengths *n*-alkanes between *n*-C_{21} and *n*-C_{35} obtained from GC analysis, following Equation 1 (Bush & McInerney, 2013). ACL_{odd} was calculated using the concentration of only odd chain lengths *n*-alkanes between *n*-C_{21} and *n*-C_{35}.

$$ACL = \sum(C_n \times n) / \sum C_n, \quad \text{(Eq. 1)}$$

where C*n* is the concentration of each *n*-alkane and n is the number of carbon atoms.

n-alkanes concentrations obtained from the GC analysis were used to determine ratios between *n*-C_{27}, *n*-C_{29}, *n*-C_{31} and *n*-C_{33} (Bush and McInerney, 2013) and for P_{aq} calculation, following Equation 2 (Ficken et al., 2000).

$$P_{aq} = \frac{(C_{23}+C_{25})}{(C_{23}+C_{25}+C_{29}+C_{31})} \quad \text{(Eq. 2)}$$

Statistical distribution, ternary diagrams and correlation were obtained from processing data with Golden Software Grapher v11.4.770 and RStudio Version 1.0.143.

3.5.2. Spatial patterns

Maps of the study area and results were generated using ArcGIS 10.1 ESRI 2011.

Precipitation data was calculated using an average precipitation map based on 30 years of daily rainfall data at a 0.25° grid resolution. This data was based on the APHRODITE data set (Asian Precipitation – Highly Resolved Observational Data Integration Towards Evaluation of Water Resources, V1101 Monsoon Asia) (Andermann et al., 2011; Yatagai et al., 2009).

4. Results

4.1. Urea adduction recovery

Samples from Rowden soil and sediment from the Godavari river basin were used to test the urea adduction method. The effect of urea adduction on *n*-alkane distributions was tested for the type of sample, concentration, the number of adductions and the effect of saponification as extraction method. Preliminary results were obtained by comparing chromatograms between original samples and samples treated with urea (Appendix A2). These results were considered for application of the method on the Godavari samples.

Recovery estimations in Table 2 show that after one round of urea treatment between 40% and 60% of the *n*-alkanes was recovered for soil sample. This recovery was lower (around 30%) when the extracts were subjected to saponification prior to purification with column chromatography. After the second and third urea adduction, the recovery was reduced by approximately 10%. Total recovery after 3 adductions showed that only 15.6% and 5.9% of the original *n*-alkane content was preserved. No changes were observed in terms of ACL between the non-adducted soil sample and the first adduction, while differences between 0.1 and 0.5 units were observed in the consecutive adductions.

Results of recovery after urea treatment for sediment samples are shown in Table 3. An important loss of *n*-alkanes was observed after the first and second urea adduction, while only a minor loss was seen after the third round of urea. Saponified samples showed the lowest recovery after adduction with only 1.3% of the original *n*-alkanes was preserved in the third round of adduction. The ACL in sediment samples exhibits a continuously increase with each adduction. The main differences are seen between the non-adducted and the first adduction, while the consecutive adductions show differences comparable to what was observed in soil samples. It must be noted that in general, sediment samples contained more UCM compared to soil samples.

The effect of concentration and *n*-alkane distributions was tested in soil samples. Differences in relative recovery, total recovery and ACL are seen in Table 2. Recovery was higher in the sample with a high concentration (A1) compared to the sample with low concentration (A2). This result was also evident when recovery of each n-alkane was estimated (Fig. 2). Fig. 2 shows that recovery in *n*-alkane distributions was higher for alkanes with longer chain lengths.

Table 2. Overview of urea adduction recovery in soil test samples. Concentration of samples A1, A2 and B are 4000µg/mg, 1000µg/mg and 2000µg/mg of extracted material, respectively.

Type of sample	Sample	Extraction method	Urea adductions	Relative recovery (%)	Total recovery (%)	ACL
Soil	A1	No saponification	No adduction			29.0
			1	62.0	62.0	29.1
			2	50.3	31.2	29.0
			3	50.2	15.6	29.1
	A2	No saponification	No adduction			29.1
			1	43.5	43.5	29.1
			2	31.1	13.5	28.7
			3	43.9	5.9	28.5
	B	Saponification	No adduction			28.8
			1	31.5	31.5	29.1

Table 3. Overview of urea adduction recovery in sediment test samples.

Type of sample	Sample	Extraction method	Urea adductions	Relative recovery (%)	Total recovery (%)	ACL
Sediment	LW1	Saponification	No adduction			28.2
			1	38.2	38.2	29.5
			2	24.2	9.2	29.5
			3	67.1	6.2	29.7
	LW2	Saponification	No adduction			27.6
			1	8.4	8.4	28.9
			2	29.5	2.5	29.1
			3	53.6	1.3	29.8

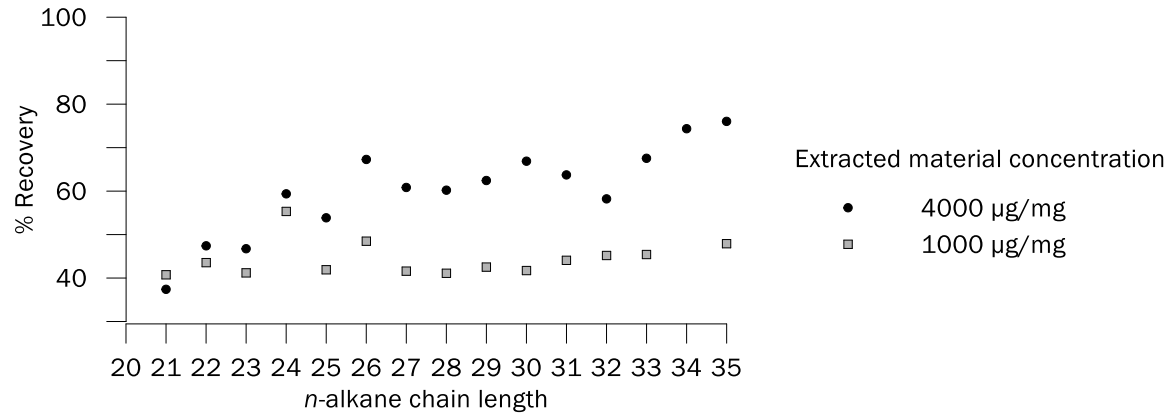

Figure 2. Urea recovery of *n*-alkanes in soil samples.

4.2. *n*-alkane distribution

A selection of soil, sediment and SPM samples was made based on spatial distribution and preliminary analysis of C content (Fig. 3). Results from adducted samples were processed to determine the relative abundance of odd and even *n*-alkanes. *n*-alkanes with chain lengths lower than 21 carbon atoms were not visible in the chromatograms, while even number *n*-alkanes were comparatively lower than odd-number *n*-alkanes. Relative abundances were calculated based on concentrations of odd *n*-alkanes between *n*-C_{21} and *n*-C_{35}. Within this range, *n*-C_{29}, *n*-C_{31} and *n*-C_{33} were the most prominent, while *n*-C_{21}, *n*-C_{23} and *n*-C_{25} were the lowest in all the sampling locations (Fig. 3).

The soils contained similarly distributed of *n*-alkanes along the river (Fig. 4), with an increasing abundance from *n*-C_{21} to *n*-C_{29}. The contribution of short chain *n*-alkanes between *n*-C_{21} and *n*-C_{27} remained below 25%, while the contribution of *n*-C_{29} ranges between 9.6% and 43.7%. In the Upper Godavari region, 3 of 4 locations had *n*-C_{29} as the main *n*-alkane, whereas in most of the other sites along the basin *n*-C_{31} was the dominating *n*-alkane. Sites in the Pranhita region contained high abundances of *n*-C_{31} and *n*-C_{33}, the latter being most abundant at G37. Soils from Indravati region showed a trend of high abundances of *n*-C_{31} and *n*-C_{33}, except for location G21, which contained high abundances of *n*-C_{29} (32.7%) and *n*-C_{27} (23.1%). In the Middle Godavari region and the Dowleiswaram reservoir, *n*-C_{31} is most abundant. Soils from the Delta region contained similar abundances of *n*-C_{21}, *n*-C_{23}, *n*-C_{25} and *n*-C_{35}, while *n*-C_{31}, *n*-C_{33} and *n*-C_{29} were the most abundant.

SPM results (Fig. 5) in the Upper Godavari region showed high abundances of *n*-C_{29}, *n*-C_{31} and *n*-C_{33}, maximising at *n*-C_{31}. In the Pranhita region, sites showed maximum abundances in *n*-C_{31} and *n*-C_{33}.

Fig. 6 illustrates that sediment has, in general, high abundances in *n*-C_{31}, followed by *n*-C_{29} and *n*-C_{33}. One location from the Upper region differs from the rest of the sites, containing low relative abundances of *n*-alkanes (between 5% and 20%). In the Indravati region, discrepancies between sediment and soil *n*-alkanes from the same sampling site were found. While alkanes in soil showed a trend of *n*-C_{29} > *n*-C_{27} > *n*-C_{31} > *n*-C_{33}, their distribution in the sediment followed *n*-C_{31} > *n*-C_{29} > *n*-C_{33} > *n*-C_{27}. Relative abundances in the Dowleiswaram Reservoir and the Delta region showed that *n*-alkanes maintain similar distributions, including what is in seen in the sediment transect TW2, TW4 and TW6.

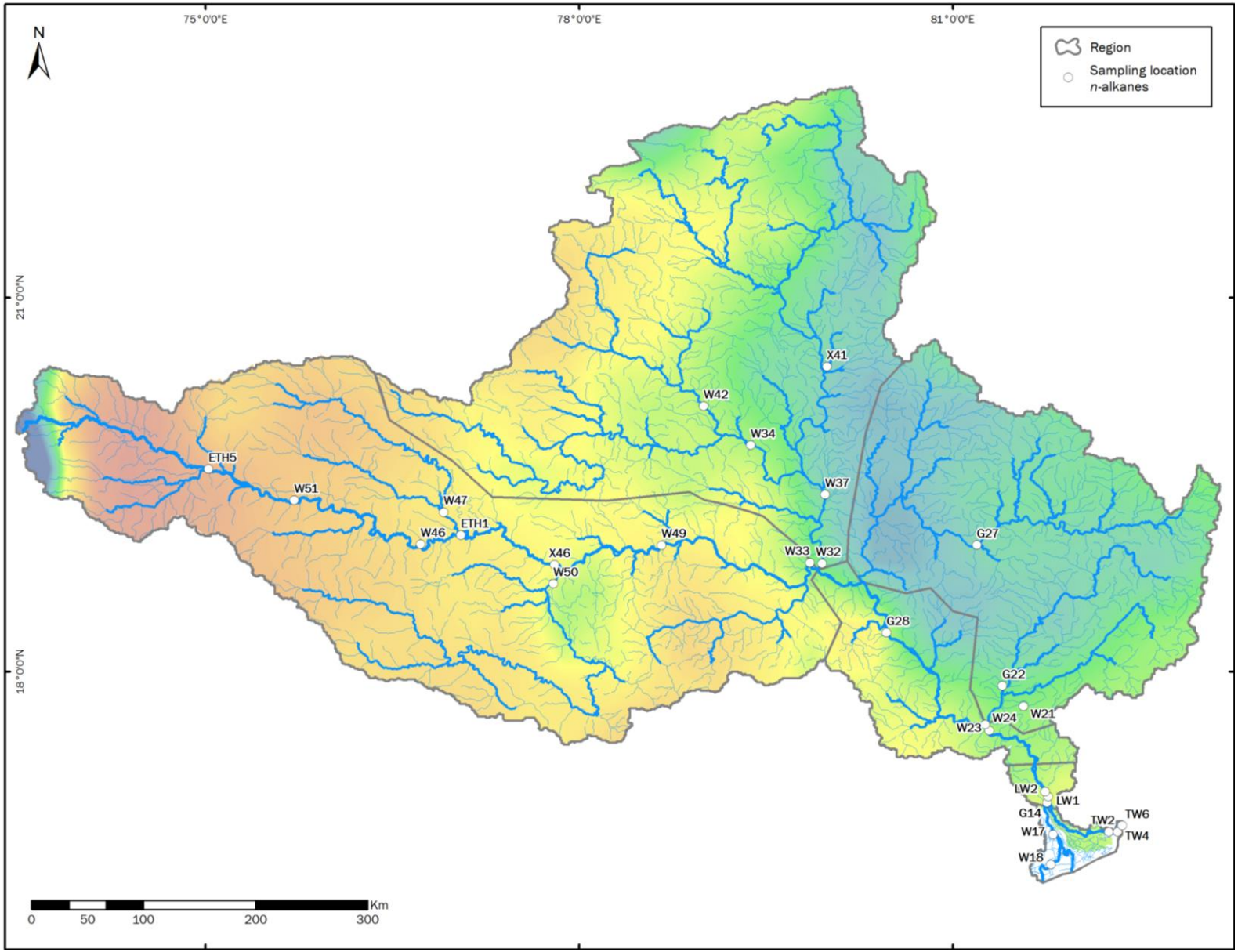

Figure 3. Location of the sites used for analysis of *n*-alkanes distributions of soil, sediment and SPM samples.

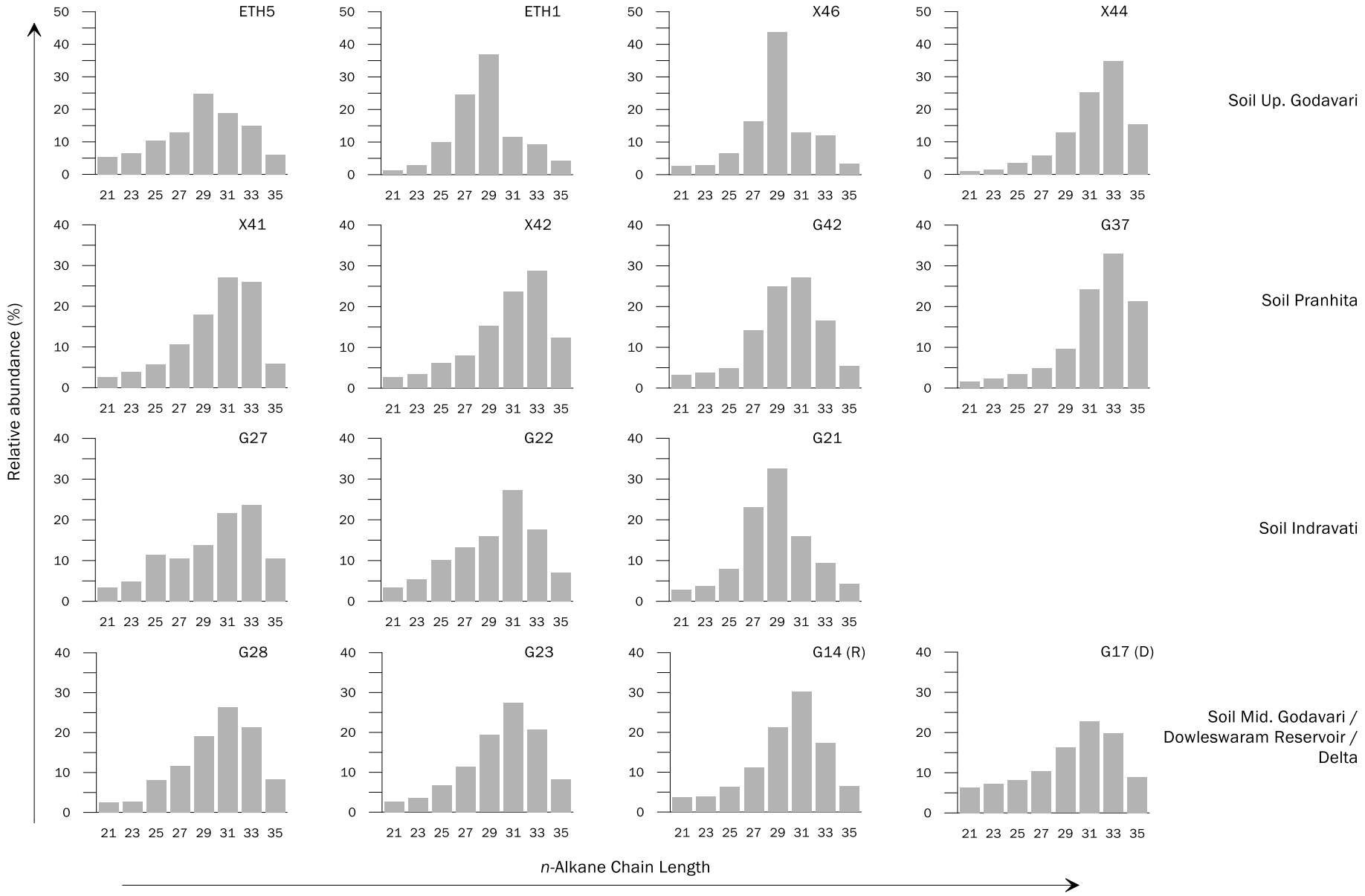

Figure 4. Average *n*-alkane distributions in soil samples based on concentrations of odd chain lengths between *n*-C_{21} and *n*-C_{35}. Relative abundances axis in the Upper Godavari region are different from the other regions.

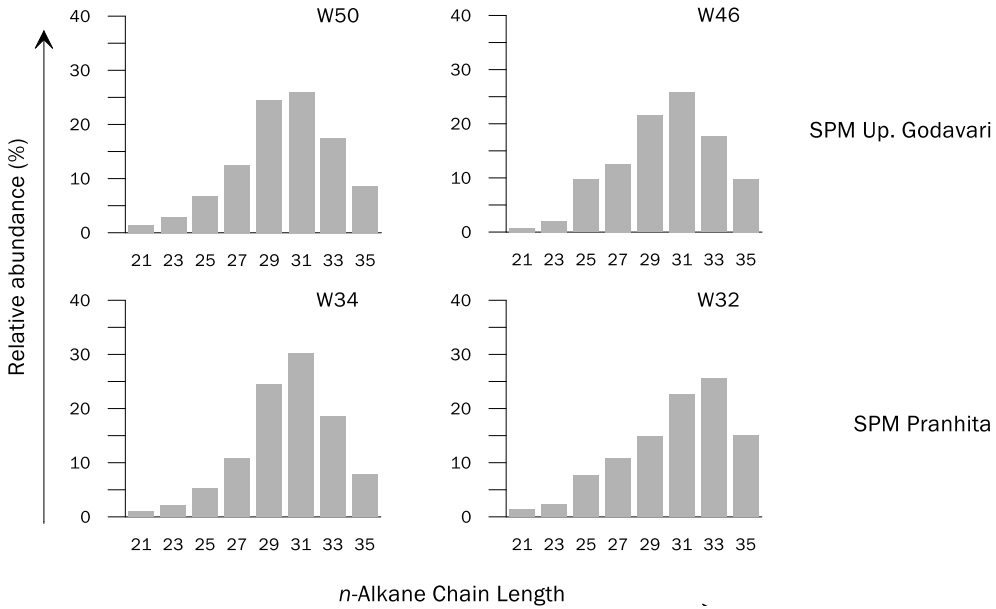

Figure 5. Average n-alkane distributions in SPM samples based on concentrations of odd chain lengths between n-C_{21} and n-C_{35}.

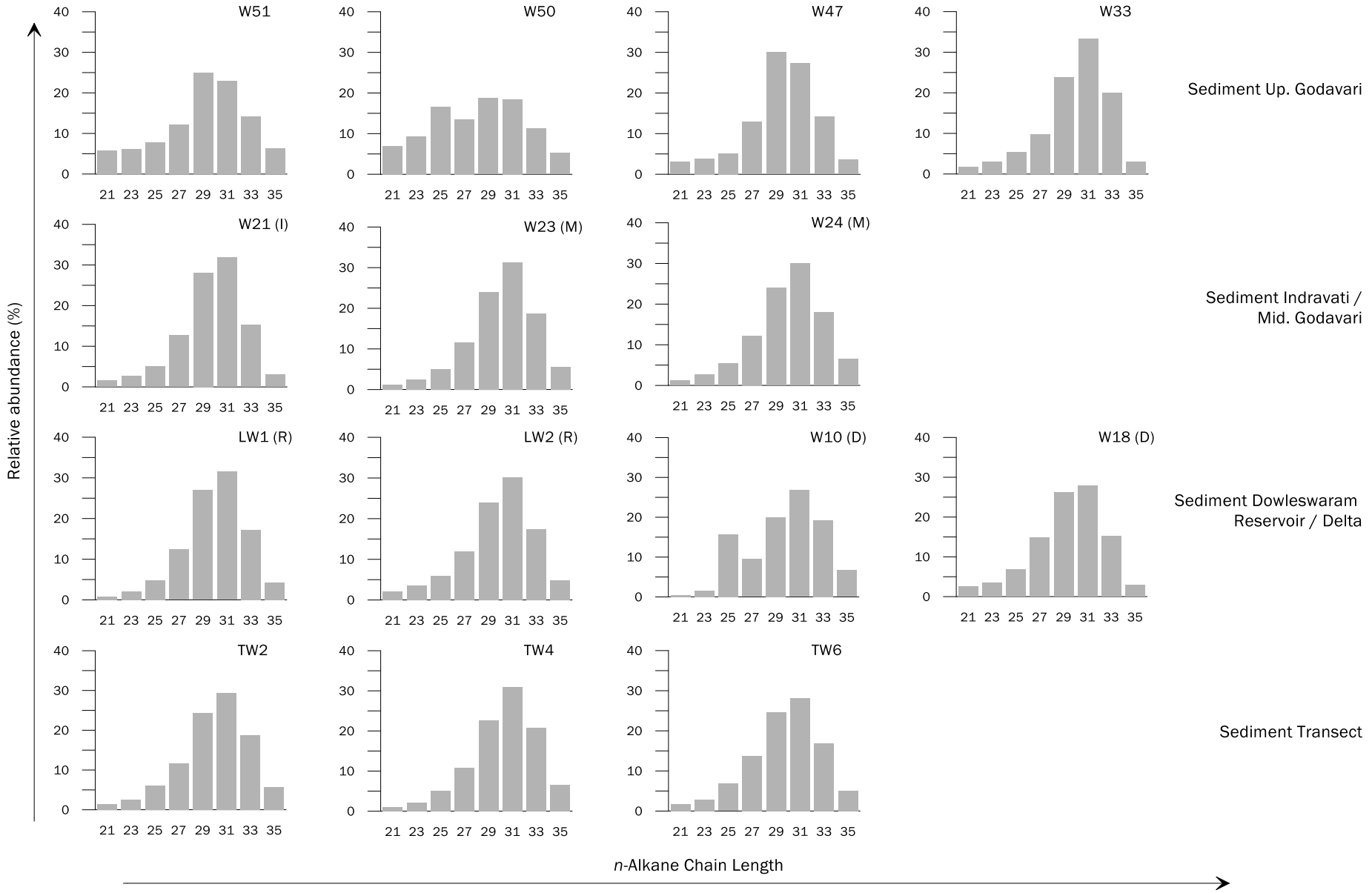

Figure 6. Average n-alkane distributions in sediment samples based on concentrations of odd chain lengths between n-C_{21} and n-C_{35}.

4.2.1. Overall chain length distribution

Th average chain length of the *n*-alkanes in each sample was calculated using the odd and even chain lengths and then only the odd chain lengths. $ACL_{odd/even}$ and ACL_{odd} are strongly correlated (r^2 = 0.98, $p < 0.05$) (Appendix A3). Since relative abundance calculation was presented with odd chain lengths between *n*-C_{21} and *n*-C_{35}, ACL_{odd} is presented in the following section.

The lowest ACL were encountered in C_3 plants (28.1 ± 0.9), followed by C_4 plants (28.4 ± 1.8), soils (29.6 ± 0.6), sediments (29.8 ± 0.8) and SPM (30.2 ± 0.3) (Fig. 7). Note that the ACL of C3 plants is based on the largest set of data and the largest range in ACL_{odd} values, from 26.2 to 30.2. While the smallest range was observed in SPM samples from only two regions. A large range in ACL_{odd} was also observed for C4 plants, which also contained the lowest ACL_{odd} (25.7). The highest ACL_{odd} value was encountered in one of the soil samples from the Pranhita region (31.6).

Average chain length distribution patterns along the different regions are shown in Fig. 8. Spatial variations can be seen between similar types of samples, in which sediments present a trend towards the Delta region, where ACL_{odd} increases. On the contrary, soils exhibited a decreasing pattern from the Pranhita region to the Delta region. Furthermore, ACL_{odd} in soils from the Upper Godavari region reflected the presence of short chain lengths around *n*-C_{29}, while SPM from the same regions tends to be higher.

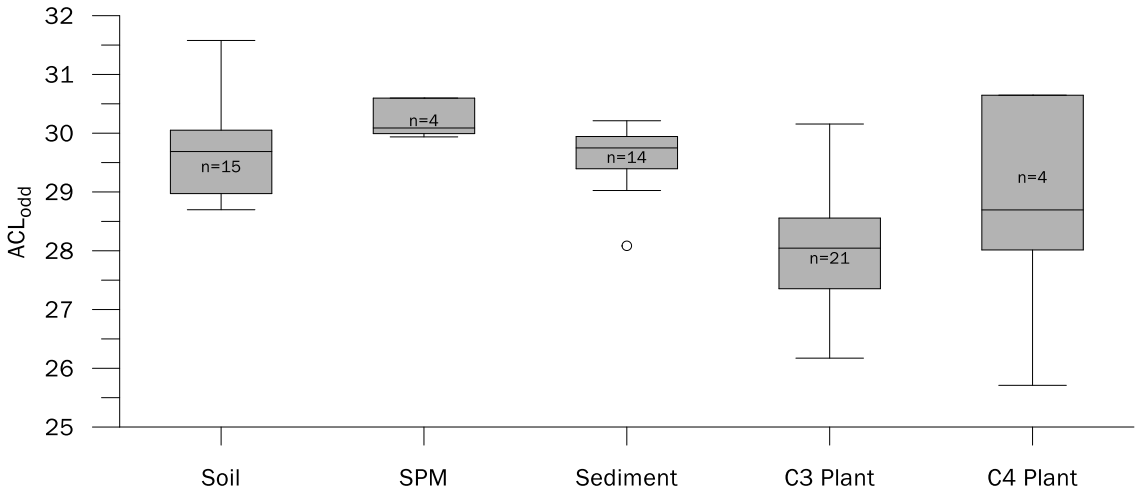

Figure 7. ACL_{odd} of the plant, soil, sediment and SPM samples among the Godavari river basin. Boxes show 25th (bottom of the box) and 75th (top of the box) percentile, while the line in the middle of the boxes represents the 50th percentile (median). The whiskers (error bars) above and below indicate the 90th and 10th percentiles, respectively. The circle indicates outliers and n are the sample size.

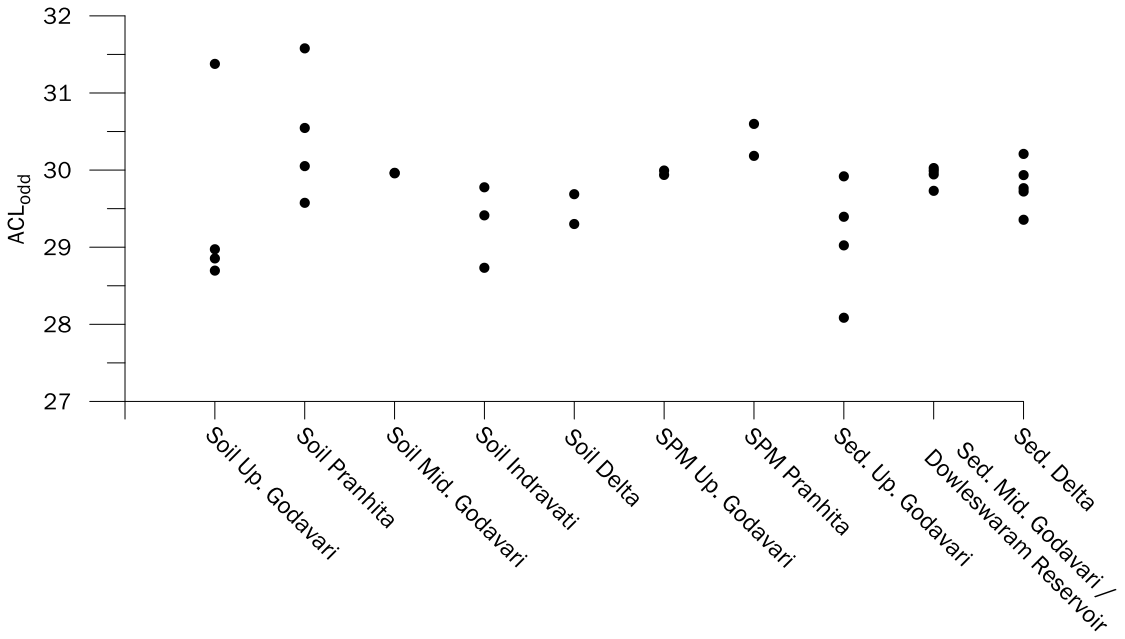

Figure 8. Average chain length (odd chain lengths only) of soils, sediments and SPM samples. The circles represent calculated ACL_{odd} of different sampling sites in each region.

4.2.2. *n*-alkane ratios

Fig. 9 shows ratios of the main *n*-alkanes distinguished in C3 and C4 plants. Soil samples incline to *n*-C_{31}, nevertheless, a few outliers with higher *n*-C_{29} ratios are visible. In general, most of the SPM and sediments contained a similar *n*-C_{27}:*n*-C_{29}:*n*-C_{31} ratio, with increasing contribution from *n*-C_{27} to *n*-C_{31}. *n*-C_{27}:*n*-C_{29}:*n*-C_{33} ratios shows that *n*-C_{33} contribution is resembling *n*-C_{27}.

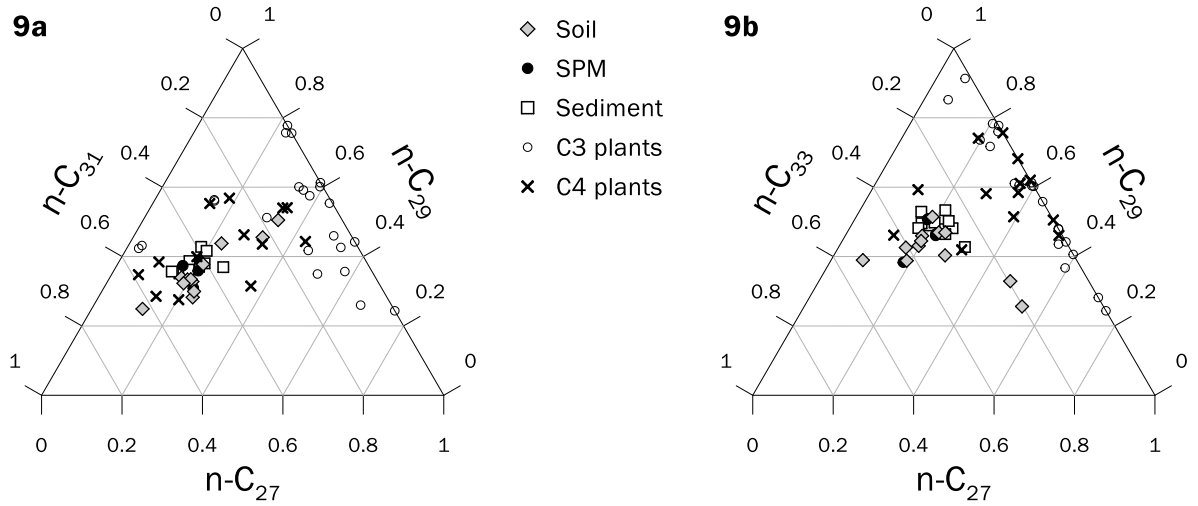

Figure 9. Ternary diagrams of *n*-alkane chain length abundances by type of sample. (a) Soil, SPM and sediment by *n*-C_{27}, *n*-C_{29} and *n*-C_{31}. (b) Soil, SPM and sediment by *n*-C_{27}, *n*-C_{29} and *n*-C_{33}.

4.2.3. Paq

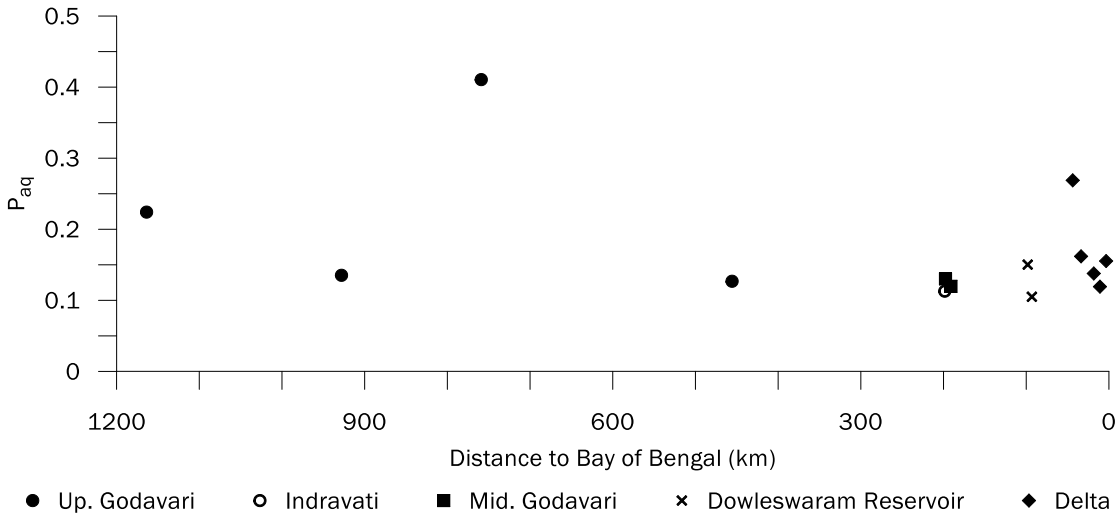

Figure 10. Spatial distribution of P_{aq} index in sediment samples along the catchment area.

P_{aq} of sediment samples ranged between 0.11 and 0.41 (Fig. 10). Two locations from the Upper Godavari region and one location in the Delta region showed P_{aq} values higher than 0.22. P_{aq} in the rest of the sampling locations varied between 0.11 and 0.16.

4.3. Compound-specific $\delta^{13}C$

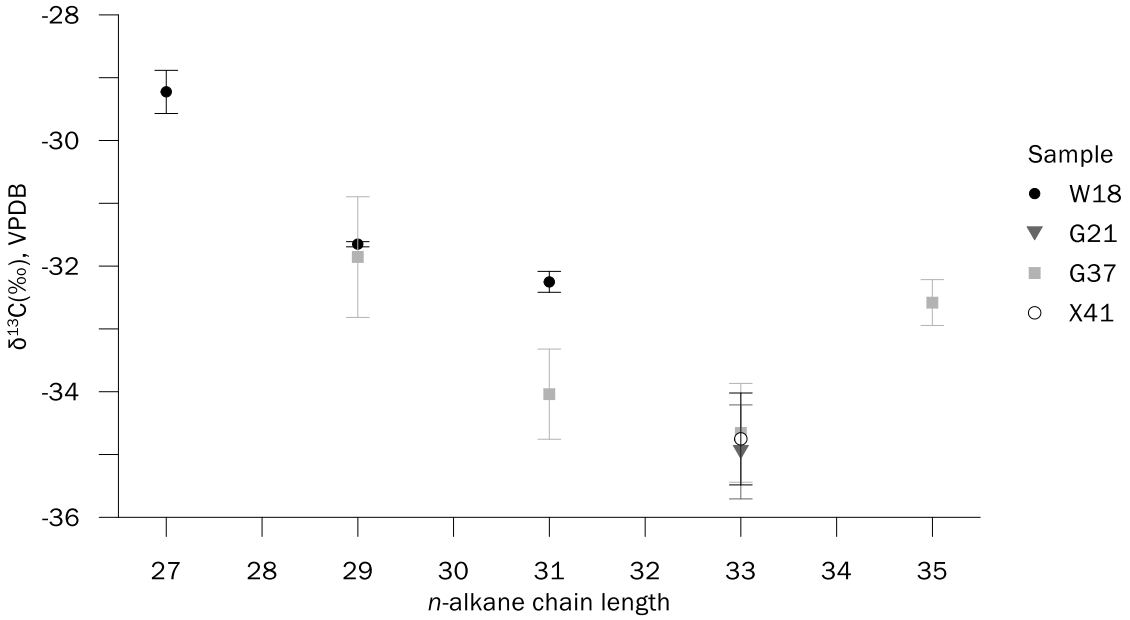

Figure 11. Compound-specific $\delta^{13}C$ in soils (G21, G37 and X41) and sediments (W18).

$\delta^{13}C$ values for alkanes *n*-C_{27}, *n*-C_{29}, *n*-C_{31}, *n*-C_{33} and *n*-C_{35} ranged between -29.2‰ and -34.7‰ (Fig. 11). The average compound-specific $\delta^{13}C$ for soil samples was -33.8 ± 1.3‰. Isotopic values in the sediment sample were more enriched compared to the soil samples, with an average of -31.0 ± 1.6‰. G37 and W18 showed tend to depleted $\delta^{13}C$ from *n*-C_{29} >

n-C_{31} > n-C_{33} and from n-C_{27} > n-C_{29} > n-C_{31}, respectively. Within the same n-alkane, n-C_{33} showed the most depleted $\delta^{13}C$ (-34.8 ± 0.2‰) in all 3 soil samples.

4.4. Bulk $\delta^{13}C$

4.4.1. Soils

Bulk carbon isotopic composition of soils and SPM are presented in Fig. 12 and 13, respectively.

Bulk $\delta^{13}C$ values in soil samples ranged between -17.9‰ and -26.3‰. Fig. 12 shows that in general, spatial trends can be observed between areas with high and low average precipitation, creating a natural boundary between the Upper Godavari region and the eastern area of the Pranhita region. More enriched signatures can be found in the Upper Godavari region, while depleted signals are observed in the eastern part of the Pranhita region, Indravati Region and Middle Godavari. Variable signatures are found in the Delta region, where the soil sample from the main distributary, G10, presents a more depleted $\delta^{13}C$ (-24.9‰) compared to G19 and G17 (-22.7‰ and -22.0‰, respectively). In general, depleted signatures are found near areas with the important contribution of C3 plants.

4.4.2. SPM

The bulk carbon isotopic composition of SPM shows distinct patterns between dry and wet seasons, where the latter presented a wider range of isotopic values. The average values for SPM in the dry season was 27.6 ± 2.0‰, while in wet season $\delta^{13}C$ was more enriched, with an average of 25.7 ± 2.0‰. Differences between the same sampling site during the dry and wet season can be seen in Fig. 13. During the wet season, SPM in the Upper region exhibited high variability in $\delta^{13}C$ values. The most enriched values (-20.0‰ and -25.9‰) were found in the Pranhita region that receives more precipitation. The Indravati region showed more depleted values compared to the Pranhita region, similar to the lower part of the Middle Godavari. Isotopic signals from the Dowleiswaram reservoir towards the Delta region were found in the range between -24‰ and -25.9‰, comparable with enriched signatures from some sampling locations of the Pranhita region.

In the dry season, a depleted signal is observed through the whole catchment compared to the wet season. Depleted values can be observed from the Upper region until the Delta region, while enriched signals can be seen in the area affected by more precipitation in the Pranhita and Indravati regions. High variability of at least 6‰ in $\delta^{13}C$ is observed from the Dowleiswaram reservoir until the Delta region.

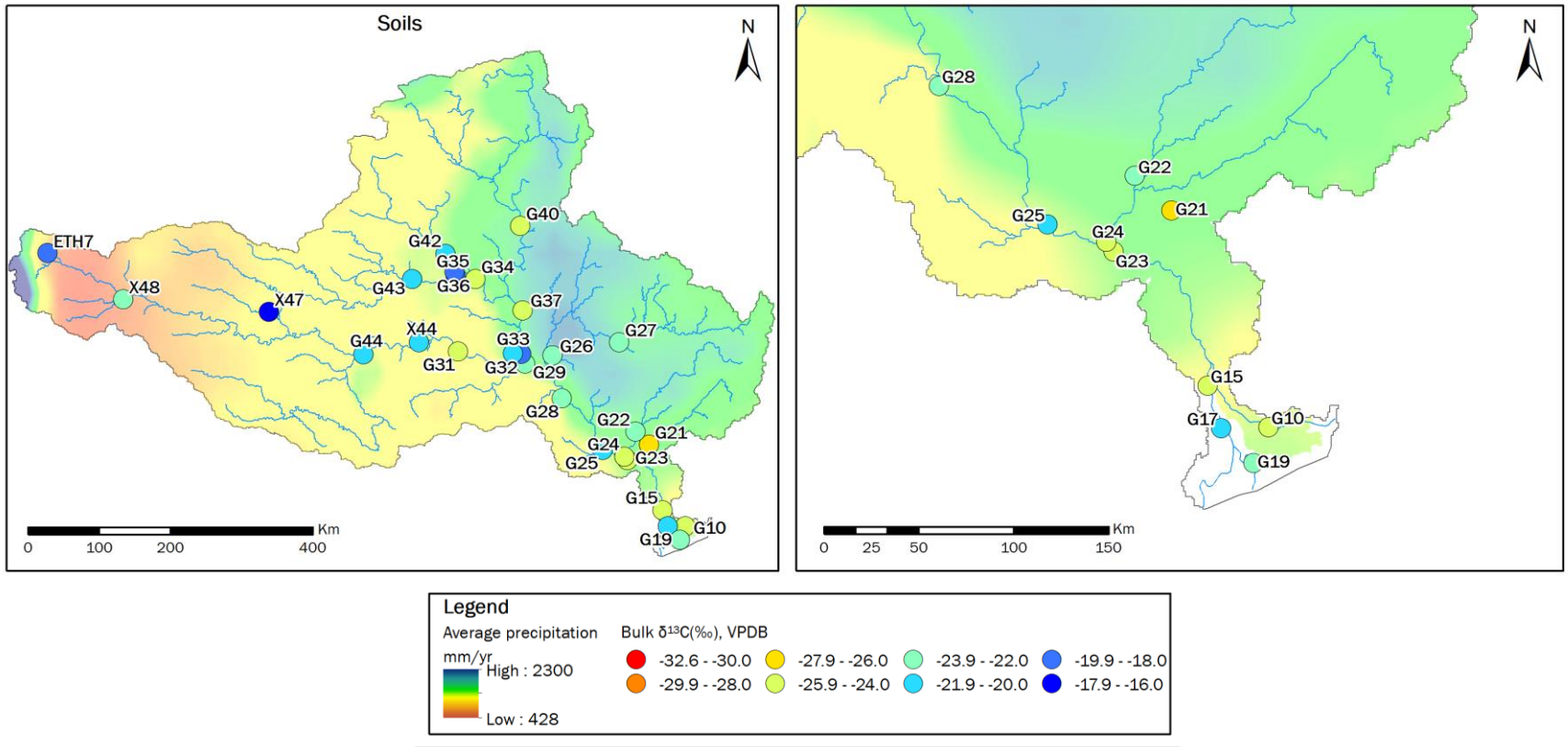

Figure 12. Carbon isotopic composition of bulk material from soil samples.

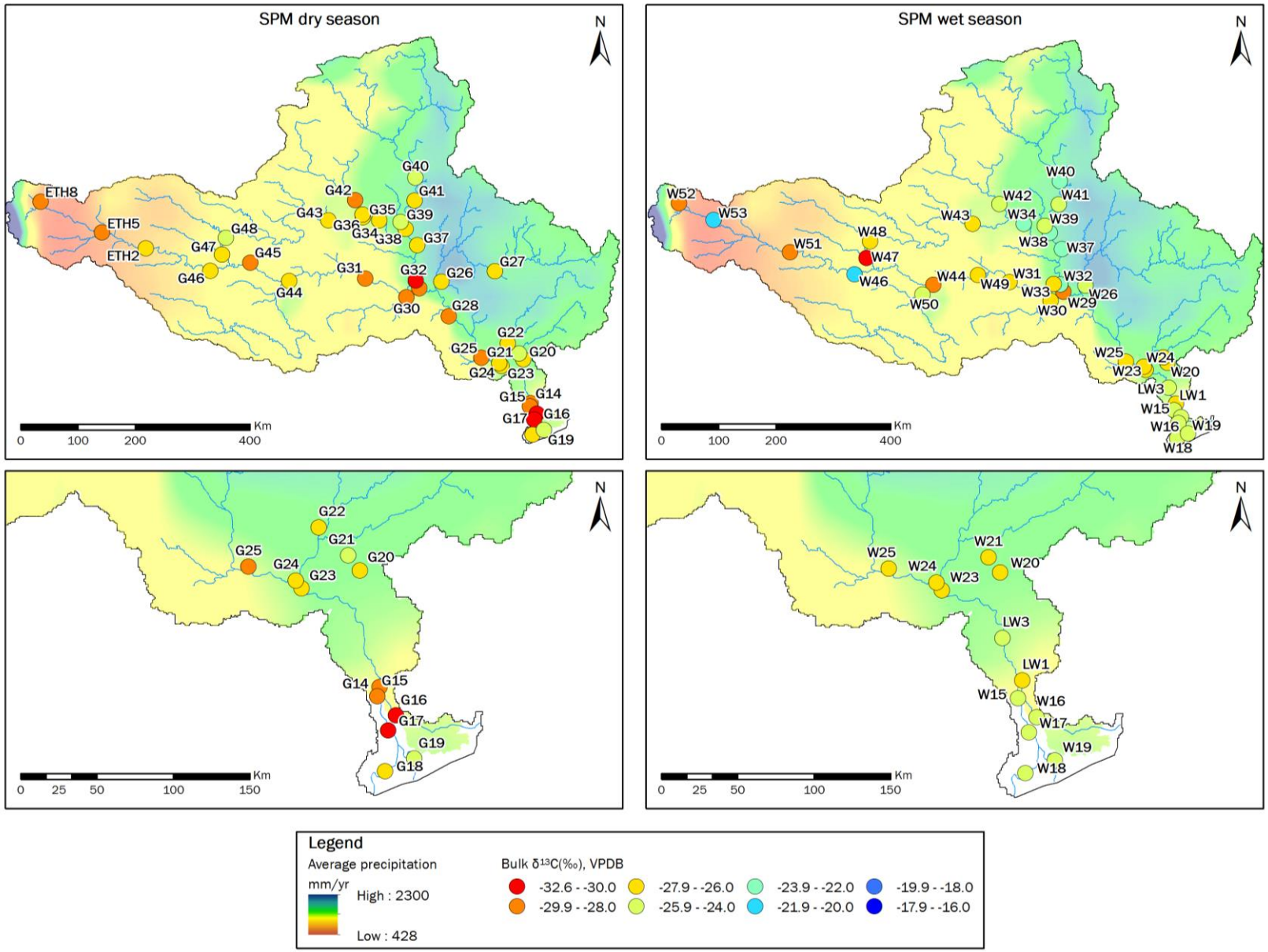

Figure 13. Carbon isotopic composition of bulk material from suspended particulate matter sample

4.4.3. Plants

The stable isotopic composition of bulk plant material plots into two distinct groups (Fig. 14), which can be linked to their metabolic pathway, i.e. C3 and C4 plants. From 102 plant samples, 83 plants from 37 different species were identified as C3 plants and 19 plants from 8 different species were identified as C4 plants.

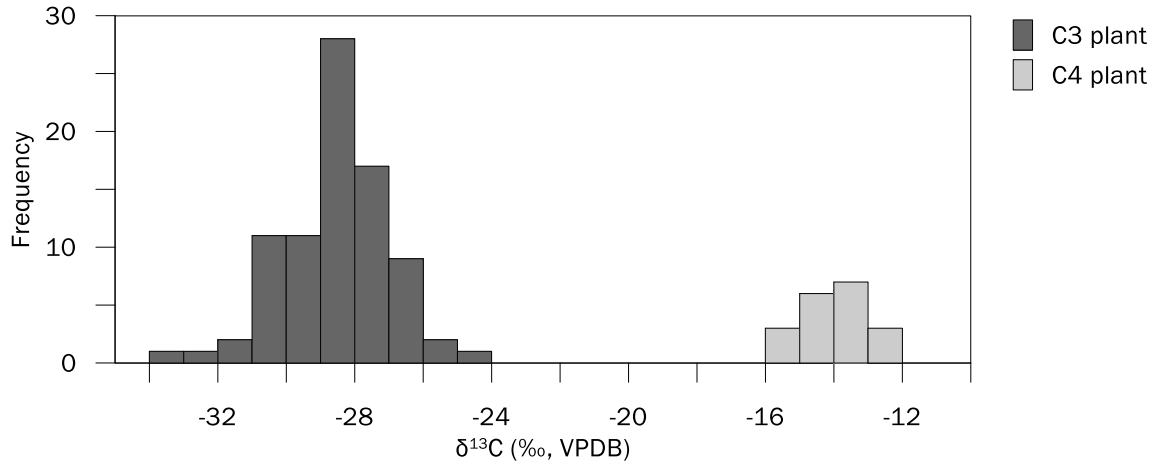

Figure 14. Frequency distribution of $\delta^{13}C$ from C3 and C4 plants along the river catchment.

C3 plants have an average value of -28.5 ± 1.6‰. Plants that were sampled more than 3 times in the catchment area are presented in Fig. 15. All 5 species of C3 plants show differences in more than 1‰ in their $\delta^{13}C$ signatures. *Acacia nilotica subsp. adstringens* and *Acacia nilotica subsp. crupressiformis* were found along the whole catchment area and showed the highest differences in $\delta^{13}C$ (at least 7‰ units). While *Alternathera sessilis* presented a low range of variability between -28‰ and -31.5‰. *Ficus semicordata* and *Ziziphus mauritiana* were found in smaller areas of the catchment, however, their isotopic signatures also exhibited important variability. In the driest area of the catchment, *Acacia nilotica subsp. adstringens* presented depleted values in locations nearby dams.

C4 plants are more enriched (Table 4) compared to C3 plants and have an average $\delta^{13}C$ value of -14.0 ± 0.7‰. The $\delta^{13}C$ values of C4 plants from the Poaceae family can vary in a range of 3‰ (Fig. 16). Outliers can be linked to sample locations close to a dam (e.g.X48).

Table 4. $\delta^{13}C$ values from bulk material of C4 plants in the study area.

Name	**Site-code**	**Region**	**$\delta^{13}C$, VPDB (‰)**
Dichanthium caricosum (L.) A. Camus	ETH1	Up. Godavari	-15.1
Cynodon dactylon (L.) Pers.	ETH8	Up. Godavari	-15.0
Cynodon dactylon (L.) Pers.	G10	Delta	-14.6
Phragmites ssp.	G16	Delta	-14.0
Poaceae	G34	Pranhita	-13.9
Dichanthium caricosum (L.) A. Camus	G42	Pranhita	-15.1
Dichanthium caricosum (L.) A. Camus	G44	Up. Godavari	-14.6
Dichanthium caricosum (L.) A. Camus	G44	Up. Godavari	-14.6
Pennisetum glaucum	G46	Up. Godavari	-13.9
Pennisetum glaucum	G46	Up. Godavari	-13.9
Saccharum officinarum	G47	Up. Godavari	-14.6
Cynodon dactylon (L.) Pers.	G48	Up. Godavari	-14.2
Cynodon dactylon (L.) Pers.	G48	Up. Godavari	-14.2
Cyperus rotundus	G48	Up. Godavari	-12.7
Sorghum vulgare	X45	Up. Godavari	-13.1
Sorghum vulgare	X46	Up. Godavari	-13.8
Zea mays	X46	Up. Godavari	-13.5
Saccharum officinarum	X48	Up. Godavari	-12.9
Dichanthium caricosum (L.) A. Camus	X48	Up. Godavari	-12.8

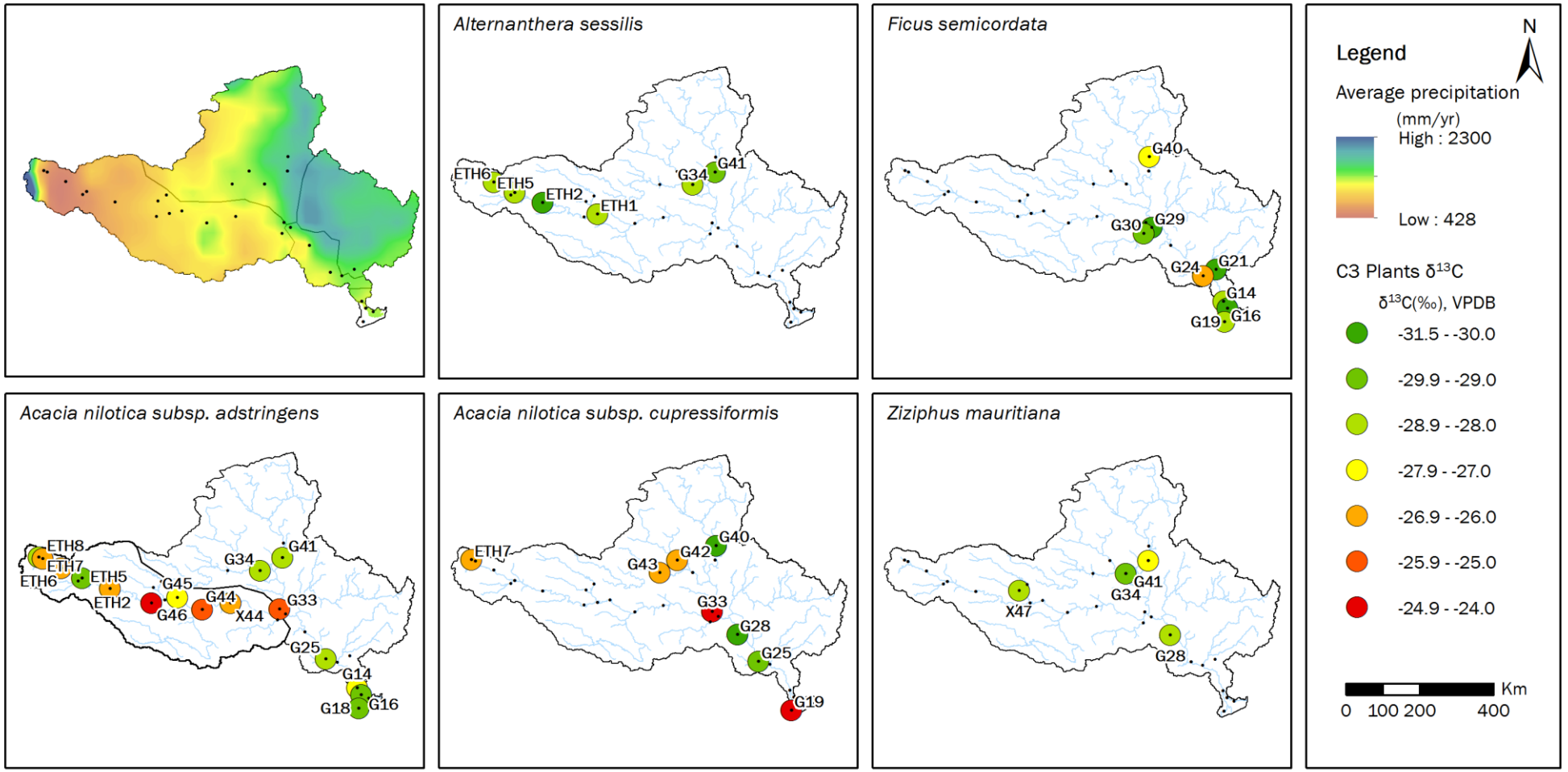

Figure 15. Isotopic composition of bulk material from C3 plants sampled more than 3 times along the catchment.

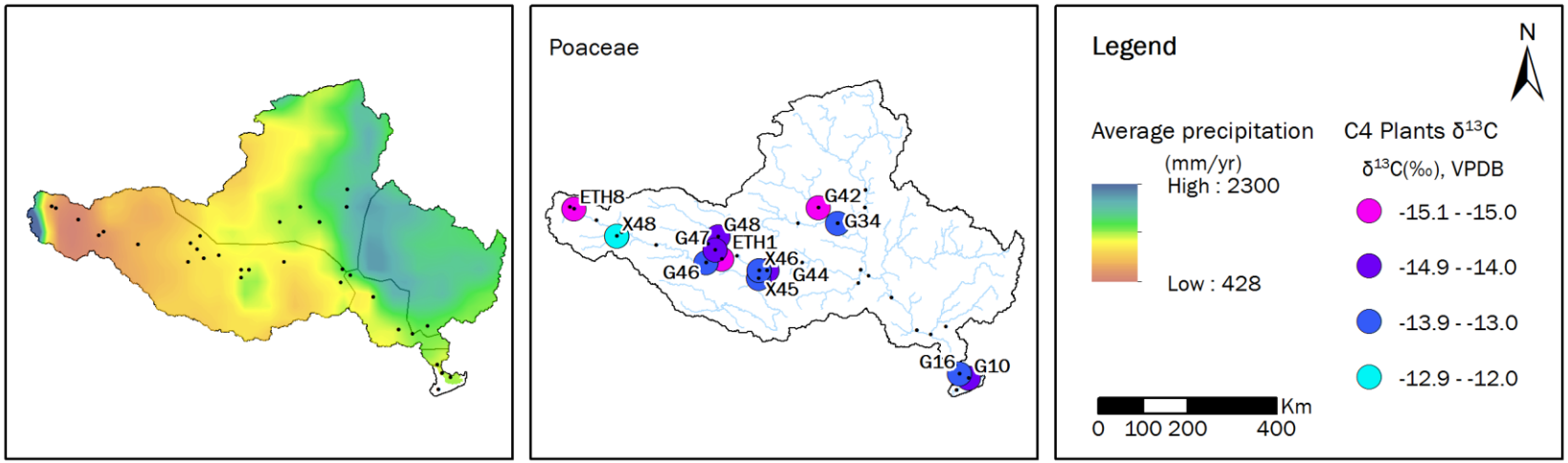

Figure 16. Isotopic composition of bulk material from C3 plants sampled more than 3 times along the catchment.

5. Discussion

5.1. Transport

5.1.1. *n*-alkanes

n-alkanes signals throughout the catchment are, in general, high in *n*-C_{29}, *n*-C_{31} and *n*-C_{33} relative abundances. Around 46% of the soil samples, 75% of SPM and 78.5% of sediment samples maximise at *n*-C_{31} (Fig. 4, 5 and 6). A typically high peak of *n*-C_{29} is observed in 3 soil samples from the Upper Godavari region (Fig. 4). Since this area receives less precipitation compared to the rest of the regions in the basin, we expected *n*-alkane distributions associated with C3 plants. Studies have associated longer chain lengths with C4 plants presence and dry-environment C3 plants (Bush and McInerney, 2015; Rommerskirchen et al., 2006b; Vogts et al., 2009), which does not match with the results obtained in the Upper Godavari region. Nonetheless, data from Martes, 2016 (Fig. 7, 9a and 9b) on *n*-alkane distributions from plants in Godavari river catchment shows that, indeed, C3 and C4 plants are dominated by *n*-C_{29}, followed by *n*-C_{27} and *n*-C_{31}. Furthermore, shifts between the most abundant *n*-alkanes in fresh/undecomposed leaves and soil have been seen earlier, showing a decrease from *n*-C_{31} and *n*-C_{29} distribution attributed to biodegradation and heterotrophic reworking (Chikaraishi and Naraoka, 2006).

Differences in *n*-alkanes distributions between soils and sediments can be attributed to *n*-alkanes that not originated from plant waxes. Previous studies have shown maximum abundances in *n*-C_{29}, *n*-C_{31} and *n*-C_{33} for terrestrial plants (Chikaraishi and Naraoka, 2003; Ficken et al., 2000), while submerged and floating plants present maximum at *n*-C_{23} and *n*-C_{25} (Ficken, et al., 2000). This evidence can explain the low relative abundances of *n*-alkanes (between 5% and 20%) in sediments at W50 (Fig. 6). In sediment samples, P_{aq} gives a good indication of the origin of the *n*-alkanes signals observed in W50, W51 and W10 (Fig. 10), associated with primary production in sites with stagnant water. While in most of the cases the range for terrestrial origin in sediment samples is around 0.1, these sites showed values in a range of 0.2 and 0.5, which is in the range informed by Ficken et al., 2000 for emergent (range 0.07 ± 0.61) and submerged and floating species (range 0.48 ± 0.94).

Similarities in average ACL values from each region (Fig. 17) are evidence of the effect of transport in *n*-alkane distributions. The main difference observed between regions responds to the effect of high contribution of *n*-C_{29} in the Upper Godavari region. While in the Pranhita region average ACL of soils and SPM are exactly the same, shifts between

soils and sediment/SPM are noticeable for the rest of the regions. ACL of sediments in the Delta region seems to indicate an integrated signal, with much of the contribution coming from the wetter area of the catchment.

Shifts between $\delta^{13}C$ of *n*-alkanes found in soil and sediments seem to indicate that even though soils are dominated by depleted signatures from presumably C3 plants, sediments from the Delta region have an integrated signal more enriched than the soils.

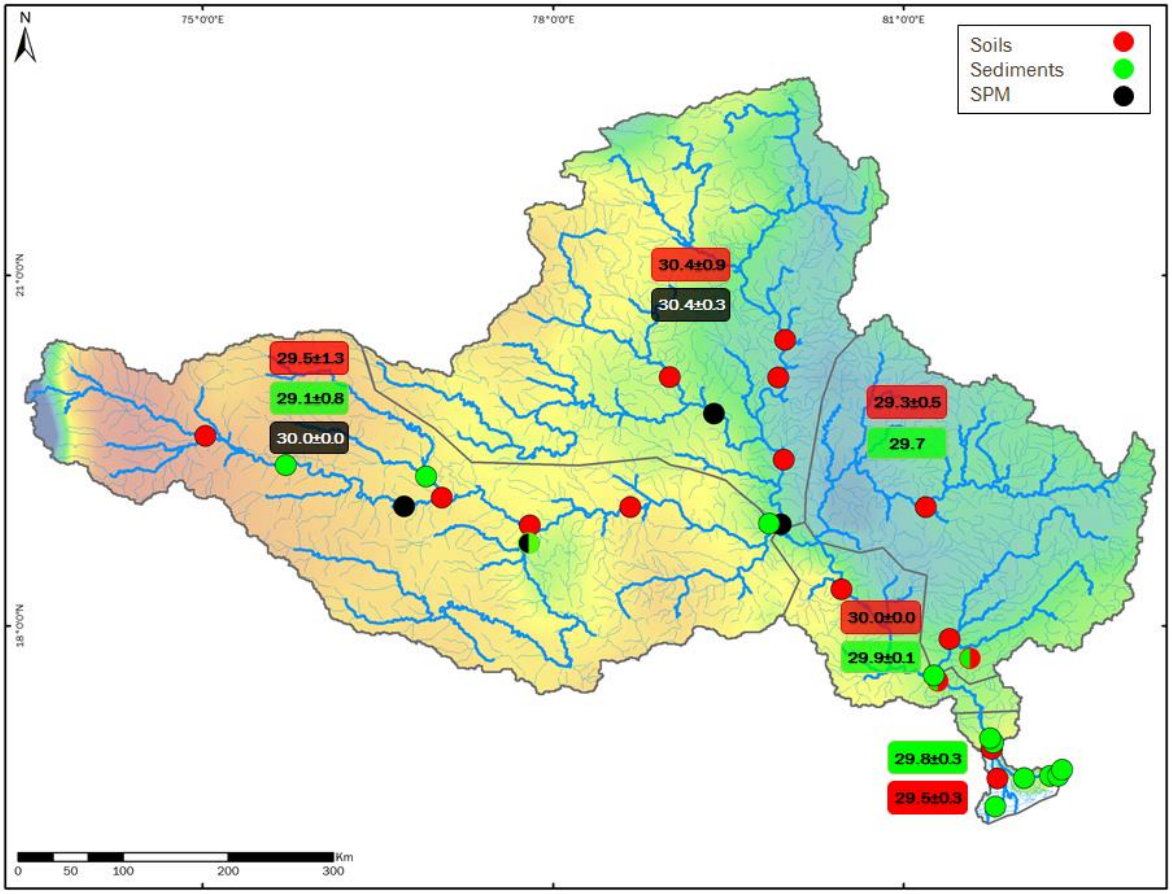

Figure 17. Average ACL per region and type of sample, with their standard deviations. Half circles symbolise sites that have 2 ACL values from different types of samples. Note that combined average values are found for the Dowleiswaram Reservoir and Delta regions.

5.1.2. Bulk $d^{13}C$

Soil $\delta^{13}C$ (Fig. 12) reveals that more enriched signatures are found in the driest areas of the catchment i.e. Upper Godavari and west of Pranhita regions. In these areas, C4 plants contribute to enriched isotopic signatures. On the contrary, depleted $\delta^{13}C$ values are present in areas that received more precipitation with depleted signatures from C3 plants, i.e. east of Pranhita Indravati, Middle Godavari, Dowleiswaram Reservoir and Delta regions. Although shifts between bulk $\delta^{13}C$ from plants and bulk soil $\delta^{13}C$ become evident, Rao et al., 2017 already demonstrated that decomposition processes show no significant

influence on the $\delta^{13}C$ data of surface soils. In its global review, carbon isotopic composition shows a wide range, yet, soil $\delta^{13}C$ in the Godavari basin has a range between -16.0‰ and -27.9‰, which follows what Rao et al., 2017 reports. Our results are also comparable to what it is been reported in soils from agricultural land in the catchment, i.e. between -19.2‰ and -23.9‰ (Pradhan et al., 2014).

Isotopic signatures present in SPM reveals the effect of precipitation in $\delta^{13}C$ transport from the soil. During dry season (Fig. 13) signals in the catchment are variable and they seem to show more contribution from the Indravati and Pranhita regions. The constant occurrence of depleted signatures implies little contribution from soils during this season. More negative $\delta^{13}C$ indicate that the signature must be coming from different sources. In situ production, can prove the provenance of depleted $\delta^{13}C$, as consequence of stagnant water. The natural flow of the river and tributaries have been historically diverted for water storage and irrigation, with 350 major/medium dams and barriers throughout the catchment (Khedkar et al., 2014). The previous report from Pradhan et al., 2014, indicate that dams and reduced rainfall caused enhancement of algal organic matter on total suspended matter and sediments from the Godavari river.

During the wet season (Fig. 13), soils prove to affect the $\delta^{13}C$ signals found in SPM. The wettest areas of the catchment contribute to more enriched signals towards the Delta region, which implies that most of the signals obtained are being transported from the Pranhita and Indravati regions. While the drier area shows more variability, which can also be explained by the effect of soil inputs and aquatic production due to damming. The effect of the dams become more evident when we analysed $\delta^{13}C$ values before and after the Dowleiswaram Reservoir. For the last 30 years, suspended sediment loads have decreased in three times in the Godavari delta (Rao et al., 2010). When the dams are open in wet season, part of this material it is transported towards the Delta, which explains why we see more enriched signatures after the dam.

Pradhan et al., 2014 reported $\delta^{13}C$ values of total suspended matter (TSM) from the Godavari river during the South West Monsoon in ranges between -22.2‰ and -24.7‰, showing heavier isotopic signatures in the upper regions than the middle and lower regions. While our results are highly variable in the Upper region, the trend seems to be opposite of what was informed by Pradhan et al., 2014.

5.2. Plants $\delta^{13}C$ signal

5.2.1. C3 or C4 vegetation

The range of bulk $\delta^{13}C$ data from C3 and C4 plants is -33.2‰ to -12.7‰ (Fig. 14). These results are consistent with reports for modern plants in a global range, i.e. −36.9‰ to −8.9‰ (Rao et al., 2017). C3 plants show a range between -33.2‰ and -24.3‰. While C4 plants have a range of -15.1‰ to -12.7‰. These results are comparable with bulk $\delta^{13}C$ data from other areas in India, i.e. Gangetic Plain. Basu et al., 2015 reports $\delta^{13}C$ values of C3 plants between -32.6‰ and -19.2‰ and from −16.6 to −10.4‰ for C4 plants. In the Godavari catchment, Pradhan et al., 2014 reports bulk $\delta^{13}C$ from C3 plants in sites located in the middle and lower basins in a range of -28.3‰ and -29.8‰. While C4 plants from upper and middle regions show values between -11.5‰ and -12.4‰. It is worth notice that even though Pradhan et al., 2014 sampled similar plants as ours, their dataset is considerably lower compared to ours and the one used in Basu et al., 2015.

Enriched signals present in C4 plants are consistent with bulk $\delta^{13}C$ observed in soil samples from the Upper Godavari region, in the range of -16.0‰ to -23.9‰. Likewise, depleted signals present in C3 plants are compatible with isotopic signatures present in the soils from Indravati, Middle and Delta regions, which exhibited ranges between -20.0‰ and -26.3‰.

5.2.2. Moisture stress

Spatial variability of bulk $\delta^{13}C$ data within the same plant species, observed in *Acacia nilotica subsp. adstringens* values from the Upper Godavari region (Fig. 18) implies the effect of moisture stress in ^{13}C fractionation. Enriched $\delta^{13}C$ observed in the driest area of the Godavari river basin can be explained by lower stomatal conductance for CO_2 in response to water stress (Farquhar and Sharkey, 1982). Isotopic values from this species in the rest of the catchment do not show high variability compared to the Upper Godavari region, and differences can be explained by more water availability in the Delta region (Fig. 15). C4 plants do not show big differences in $\delta^{13}C$ (Fig. 16), implying that moisture stress does not affect these plants in the same way as C3 plants. It has been noted that due to the efficiency in carbon fixation mechanisms, C4 have shown little environmental variability in $\delta^{13}C$ (Ehleringer et al., 1997; Marshall et al., 2007). The effect of this moisture stress on C3 plant signals can also explain the enrichment of bulk $\delta^{13}C$ observed in soils. Studies have reported end-member values for C3 plants in mid-latitude and equatorial vegetation of -28.5‰ (Kohn, 2010) and -29.5‰ for the southcentral Gangetic

Plain, India (Agrawal et al., 2012). These results are comparable to our end-members of C3 plants for the Delta region is -28.5 ± 1.2 ‰.

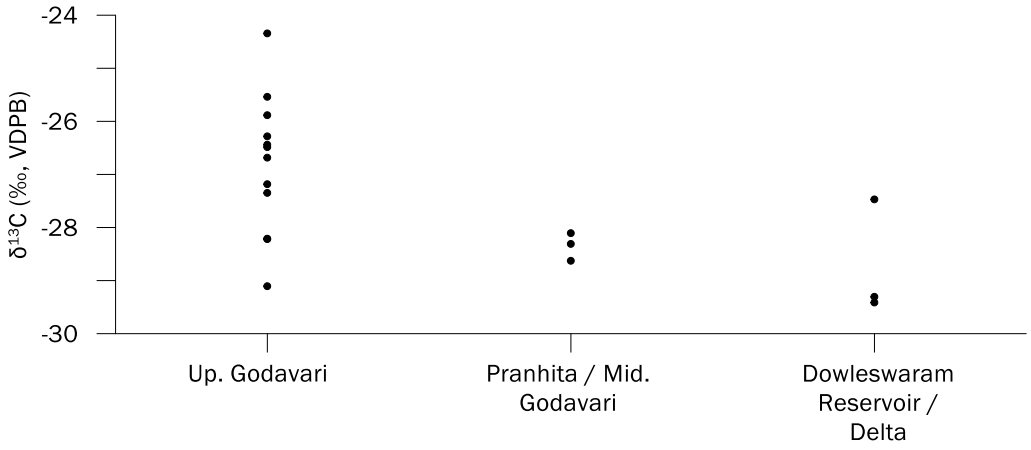

Figure 18. Spatial variability of $\delta^{13}C$ in *Acacia nilotica subsp. adstringens.*

5.3. Implications

Rao et al., 2015 reports $\delta^{13}C$ values from plant material in core sites studied in the Godavari delta, which is in a range between -20.6‰ and -29.1‰. Ponton et al., 2012 obtained $\delta^{13}C$ values in the range between -23‰ and -30‰ from a sediment core recovered close to the Godavari river mouth. Additionally, Ponton et al., 2012 calculated isotopic end-members of -37.7 ± 1.8‰ and -21.1 ± 1.4‰ for C3 and C4 plants, respectively, obtained from $\delta^{13}C$ measurements of n-alkanoic acids isolated from different plant species (Chikaraishi et al., 2004). Considering that our results on end-members for C3 plants are evidence of lower $\delta^{13}C$ values compared to global trends, we postulate that end-members in sedimentary records are being overestimated.

6. Conclusions

This study presents the *n*-alkane distribution in soil, sediments, SPM and plant samples, as well as bulk $\delta^{13}C$ distribution in soil, SPM and plants from the Godavari river basin, India. In terms of *n*-alkanes distributions, odd chain lengths between *n*-C_{27} and *n*-C_{31} were observed to dominate most of the environments along the catchment area. Using average chain lengths, we found that *n*-alkanes from the wetter area of the catchment are being transported to the Delta. Ratios between *n*-C_{27}, *n*-C_{29}, *n*-C_{31} and *n*-C_{33} contributed to elucidate that soil, sediment and SPM *n*-alkane distributions thought the catchment are similar. The Paq index indicated in situ production in sediments from certain locations of the river basin.

The carbon isotopic composition in soils shows that the type of vegetation dominating the region is a large control. The Upper Godavari region presented the lowest precipitation in the basin, influencing the presence of C4 plants and signifying in enriched soil bulk $\delta^{13}C$. Catchment areas with high precipitation and high C3 plants production were dominated by depleted soils. Nevertheless, heavier $\delta^{13}C$ values for C3 plants in the upper catchment suggests that moisture stress affects carbon fractionation, and implies that soils enriched in ^{13}C do not necessarily reflect C4 vegetation.

Isotopic signatures in SPM during wet season shows that $\delta^{13}C$ from soils is transported, mainly from signals coming from the wetter area of the catchment, i.e. east of the Pranhita region and the Indravati region. The signal discharged in the Delta region seems to be heavily influenced by the dam in the Dowleiswaram reservoir, which appears to indicate the effect of accumulation in the sediments and the discharge of a long-term signal. During dry season $\delta^{13}C$ values found in the catchment are represented by aquatic production.

Even though bulk $\delta^{13}C$ signals have multiple sources of organic matter, *n*-alkanes distributions show the same trends on transport, indicating that our conclusions are robust.

Acknowledgments

At first, I would like to thank dr. Francien Peterse and Frédérique Kirkels MSc. for introducing me to this project and for their guidance, encouragement and support throughout my thesis. I would also once again like to extend my gratitude to Frédérique for her constant help during every step of this thesis and for always being available to answer my questions.

In addition, I would like to thank the laboratory staff, Klaas Nierop, Dominika Kasjaniuk and Anita van Leeuwen-Tolboom for their continuous help and orientation during laboratory work. Moreover, I would like to acknowledge the National Herbarium of the Netherlands (Leiden) for supplying information about the identification of species obtained in the field. To Ronald van Bommel and Marcel van der Meer from the Royal Netherlands Institute for Sea Research (NIOZ) for the isotopic analysis of our samples.

I would also like to thank Constanza Maass for her help in the representation of results with GIS and her continuous moral support throughout this thesis.

Finally, thanks to my fellow classmates, friends and family for their constant support and encouragement during these past two years of Master.

This project and Master were funded by NOW Veni Grant #863.13.016 to Francien Peterse and Becas Chile (Conicyt), respectively.

References

Andermann, C., Bonnet, S., & Gloaguen, R. (2011). Evaluation of precipitation data sets along the Himalayan front. *Geochemistry, Geophysics, Geosystems*, *12*(7).

Basu, S., Agrawal, S., Sanyal, P., Mahato, P., Kumar, S., & Sarkar, A. (2015). Carbon isotopic ratios of modern C3–C4 plants from the Gangetic Plain, India and its implications to paleovegetational reconstruction. *Palaeogeography, Palaeoclimatology, Palaeoecology*, *440*, 22-32.

Bi, X., Sheng, G., Liu, X., Li, C., & Fu, J. (2005). Molecular and carbon and hydrogen isotopic composition of n-alkanes in plant leaf waxes. *Organic Geochemistry*, *36*(10), 1405-1417.

Biksham, G., & Subramanian, V. (1988). Nature of solute transport in the Godavari basin, India. *Journal of Hydrology*, *103*(3-4), 375-392.

Biksham, G., & Subramanian, V. (1988). Sediment transport of the Godavari River basin and its controlling factors. *Journal of Hydrology*, *101*(1-4), 275-290.

Bush, R. T., & McInerney, F. A. (2015). Influence of temperature and C4 abundance on n-alkane chain length distributions across the central USA. *Organic Geochemistry*, *79*, 65-73.

Carr, A. S., Boom, A., Grimes, H. L., Chase, B. M., Meadows, M. E., & Harris, A. (2014). Leaf wax n-alkane distributions in arid zone South African flora: environmental controls, chemotaxonomy and palaeoecological implications. *Organic Geochemistry*, 67, 72-84.

Castañeda, I. S., & Schouten, S. (2011). A review of molecular organic proxies for examining modern and ancient lacustrine environments. *Quaternary Science Reviews*, *30(21)*, 2851-2891.

Chikaraishi, Y., & Naraoka, H. (2003). Compound-specific δD–δ^{13}C analyses of n-alkanes extracted from terrestrial and aquatic plants. *Phytochemistry*, *63*(3), 361-371.

Chikaraishi, Y., Naraoka, H., & Poulson, S. R. (2004). Hydrogen and carbon isotopic fractionations of lipid biosynthesis among terrestrial (C3, C4 and CAM) and aquatic plants. *Phytochemistry*, *65*(10), 1369-1381.

Chikaraishi, Y., & Naraoka, H. (2006). Carbon and hydrogen isotope variation of plant biomarkers in a plant–soil system. *Chemical Geology*, *231*(3), 190-202.

Collister, J. W., Rieley, G., Stern, B., Eglinton, G., & Fry, B. (1994). Compound-specific δ 13C analyses of leaf lipids from plants with differing carbon dioxide metabolisms. *Organic Geochemistry*, *21*(6-7), 619-627.

Conte, M. H., Weber, J. C., Carlson, P. J., & Flanagan, L. B. (2003). Molecular and carbon isotopic composition of leaf wax in vegetation and aerosols in a northern prairie ecosystem. *Oecologia*, *135*(1), 67-77.

Cranwell, P. A., Eglinton, G., & Robinson, N. (1987). Lipids of aquatic organisms as potential contributors to lacustrine sediments—II. *Organic Geochemistry, 11(6),* 513-527.

Deines, P. (1980). The isotopic composition of reduced organic carbon. *Handbook of Environmental Isotope Geochemistry. The Terrestrial Environment*, *1*, 329-406.

Diefendorf, A. F., Mueller, K. E., Wing, S. L., Koch, P. L., & Freeman, K. H. (2010). Global patterns in leaf 13C discrimination and implications for studies of past and future climate. *Proceedings of the National Academy of Sciences*, *107*(13), 5738-5743.

Eglinton, T. I., & Eglinton, G. (2008). Molecular proxies for paleoclimatology. *Earth and Planetary Science Letters*, *275*(1), 1-16.

Eglinton, G., & Hamilton, R. J. (1967). Leaf epicuticular waxes. *Science, 156(3780),* 1322-1335.

Ehleringer, J. R., Cerling, T. E., & Helliker, B. R. (1997). C4 photosynthesis, atmospheric CO2, and climate. *Oecologia*, *112*(3), 285-299.

Farquhar, G. D., Ehleringer, J. R., & Hubick, K. T. (1989). Carbon isotope discrimination and photosynthesis. *Annual review of plant biology*, *40*(1), 503-537.

Ficken, K. J., Li, B., Swain, D. L., & Eglinton, G. (2000). An n-alkane proxy for the sedimentary input of submerged/floating freshwater aquatic macrophytes. *Organic geochemistry, 31(7),* 745-749.

Freeman, K. H., & Colarusso, L. A. (2001). Molecular and isotopic records of C4 grassland expansion in the late Miocene. *Geochimica et Cosmochimica Acta, 65(9),* 1439-1454.

Frysinger, G. S., Gaines, R. B., Xu, L., & Reddy, C. M. (2003). Resolving the unresolved complex mixture in petroleum-contaminated sediments. *Environmental science & technology, 37(8),* 1653-1662.

Giger, W., Schaffner, C., & Wakeham, S. G. (1980). Aliphatic and olefinic hydrocarbons in recent sediments of Greifensee, Switzerland. *Geochimica et Cosmochimica Acta*, *44*(1), 119-129.

Gupta, L. P., Subramanian, V., & Ittekkot, V. (1997). Biogeochemistry of particulate organic matter transported by the Godavari River, India. *Biogeochemistry, 38(2),* 103-128.

JoVE Science Education Database. Essentials of Earth Science. Removal of Branched and Cyclic Compounds by Urea Adduction for Uk'37 Paleothermometry. JoVE, Cambridge, MA, (2017).

Kahmen, A., Hoffmann, B., Schefuß, E., Arndt, S. K., Cernusak, L. A., West, J. B., & Sachse, D. (2013). Leaf water deuterium enrichment shapes leaf wax *n*-alkane δD values of angiosperm plants II: Observational evidence and global implications. *Geochimica et Cosmochimica Acta, 111,* 50-63.

Khedkar, G. D., Lutzky, S., Rathod, S., Kalyankar, A., & David, L. (2014). A dual role of dams in fragmentation and support of fish diversity across the Godavari River basin in India. *Ecohydrology*, *7*(6), 1560-1573.

Kohn, M. J. (2010). Carbon isotope compositions of terrestrial C3 plants as indicators of (paleo) ecology and (paleo) climate. *Proceedings of the National Academy of Sciences*, *107*(46), 19691-19695.

Komada, T., Anderson, M. R., & Dorfmeier, C. L. (2008). Carbonate removal from coastal sediments for the determination of organic carbon and its isotopic signatures, δ13C and Δ14C: comparison of fumigation and direct acidification by hydrochloric acid. *Limnology and Oceanography: Methods*, *6*(6), 254-262.

Marshall, J. D., Brooks, J. R., & Lajtha, K. (2007). Sources of variation in the stable isotopic composition of plants. *Stable isotopes in ecology and environmental science*, *2*, 22-60.

Martes, C.R.T. (2015). n-Alkanes as tracer for plant-derived organic carbon in the Godavari river system. Master Thesis, Utrecht University.

Meyers, P. A. (2003). Applications of organic geochemistry to paleolimnological reconstructions: a summary of examples from the Laurentian Great Lakes. *Organic geochemistry*, *34*(2), 261-289.

Meyers, P. A., & Ishiwatari, R. (1993). Lacustrine organic geochemistry—an overview of indicators of organic matter sources and diagenesis in lake sediments. *Organic geochemistry, 20(7),* 867-900.

Nwadinigwe, C. A., & Nwobodo, I. O. (1994). Analysis of *n*-paraffins in light crudes: molecular sieve and urea adduction techniques revisited. *Fuel, 73(5),* 779-782.

O'Leary, M. H. (1981). Carbon isotope fractionation in plants. *Phytochemistry*, *20*(4), 553-567.

O'Leary, M. H. (1988). Carbon isotopes in photosynthesis. *Bioscience*, *38*(5), 328-336.

Panda, D. K., Kumar, A., & Mohanty, S. (2011). Recent trends in sediment load of the tropical (Peninsular) river basins of India. *Global and Planetary Change*, *75*(3), 108-118.

Ponton, C., Giosan, L., Eglinton, T. I., Fuller, D. Q., Johnson, J. E., Kumar, P., & Collett, T. S. (2012). Holocene aridification of India. *Geophysical Research Letters*, *39*(3).

Pradhan, U. K., Wu, Y., Shirodkar, P. V., Zhang, J., & Zhang, G. (2014). Multi-proxy evidence for compositional change of organic matter in the largest tropical (peninsular) river basin of India. *Journal of Hydrology, 519*, 999-1009.

Rao, K. N., Subraelu, P., Kumar, K. C. V., Demudu, G., Malini, B. H., & Rajawat, A. S. (2010). Impacts of sediment retention by dams on delta shoreline recession: evidences from the Krishna and Godavari deltas, India. *Earth Surface Processes and Landforms*, *35*(7), 817-827.

Rao, K. N., Saito, Y., Nagakumar, K. C. V., Demudu, G., Rajawat, A. S., Kubo, S., & Li, Z. (2015). Palaeogeography and evolution of the Godavari delta, east coast of India during the Holocene: an example of wave-dominated and fan-delta settings. *Palaeogeography, Palaeoclimatology, Palaeoecology*, *440*, 213-233.

Rao, Z., Guo, W., Cao, J., Shi, F., Jiang, H., & Li, C. (2017). The relationship between the stable carbon isotopic composition of modern plants and surface soils and climate: A global review. *Earth-Science Reviews*, *165*, 110-119.

Rommerskirchen, F., Eglinton, G., Dupont, L., Güntner, U., Wenzel, C., & Rullkötter, J. (2003). A north to south transect of Holocene southeast Atlantic continental margin sediments: Relationship between aerosol transport and compound-specific δ13C land plant biomarker and pollen records. *Geochemistry, Geophysics, Geosystems*, *4*(12).

Rommerskirchen, F., Plader, A., Eglinton, G., Chikaraishi, Y., & Rullkötter, J. (2006). Chemotaxonomic significance of distribution and stable carbon isotopic composition of long-chain alkanes and alkan-1-ols in C4 grass waxes. *Organic Geochemistry*, *37*(10), 1303-1332.

Sachse, D., Radke, J., & Gleixner, G. (2006). δD values of individual *n*-alkanes from terrestrial plants along a climatic gradient–Implications for the sedimentary biomarker record. *Organic Geochemistry, 37(4),* 469-483.

Sage, R. F., Wedin, D. A., & Li, M. (1998). The biogeography of C4 photosynthesis: patterns and controlling factors. *C4 Plant Biology*, 313.

Vogts, A., Moossen, H., Rommerskirchen, F., & Rullkötter, J. (2009). Distribution patterns and stable carbon isotopic composition of alkanes and alkan-1-ols from plant waxes of African rain forest and savanna C 3 species. *Organic Geochemistry*, *40*(10), 1037-1054.

Voort, T. S. V. D., Hagedorn, F., McIntyre, C., Zell, C., Walthert, L., Schleppi, P., ... & Eglinton, T. I. (2016). Variability in 14 C contents of soil organic matter at the plot and regional scale across climatic and geologic gradients. *Biogeosciences*, *13*(11), 3427-3439.

Yatagai, A., Kamiguchi, K., Arakawa, O., Hamada, A., Yasutomi, N., & Kitoh, A. (2012). APHRODITE: Constructing a long-term daily gridded precipitation dataset for Asia based on a dense network of rain gauges. *Bulletin of the American Meteorological Society*, *93*(9), 1401-1415.

Appendix

A1. Urea adduction protocol

To separate straight chain hydrocarbons from branched and cyclic components an optimized procedure has been developed. Depending on the sample matrix and expected results, more than one urea adduction might be needed. In this procedure, 2 urea adductions are recommended.

- Combust borosilicate glass pipettes and 4 mL vials.
- Pre-weight vials for non-adduct and adduct fractions.
- Dissolve apolar fraction in 1.5 mL of DCM/Hexane 2/1 v/v.
- Add 1.5 mL of urea in MeOH (100 mg/mL).
- Freeze for 30 minutes to let the crystals form.
- Dry under N_2 (start with a gentle flow to avoid clusters of crystals around the vial).
- Add 5x approximately 0.8 mL of hexane into the vial. Turn the vial to allow contact between the solvent and the crystals. Recover the hexane with a pipette (avoid getting crystals in the pipette) and transfer into a pre-weighted vial (non-adduct fraction).
- Add 2x 1 mL of ultra-pure water through the previously used pipette into the vial (discard the pipette after use). Use vortex to complete the dissolution. If hexane was left from the previous step you will observe a thin layer on top of the water.
- Add 5x approximately 0.8 mL of hexane and shake the vial with a vortex. In each addition wait for approximately 1 minute to let the phases form. Collect the upper layer in the adduct fraction pre-weighted vial.
- Gently dry the non-adduct and adduct fractions under N_2 and weigh the vials.
- After this step, there will be three fractions: non-adduct, adduct and urea/water leftover. This last fraction should be discarded in the appropriate waste bin (halogen-containing organic solvents).
- Repeat the steps on the adducted fraction to ensure all non-adduct material is removed. If the original background is too high repeat the procedure once more.

Note: Ensure that all the solvent is completely dry before rinsing with hexane, otherwise urea crystals can move through the pipette.

A2. Chromatograms of sediment samples tested for urea recovery.

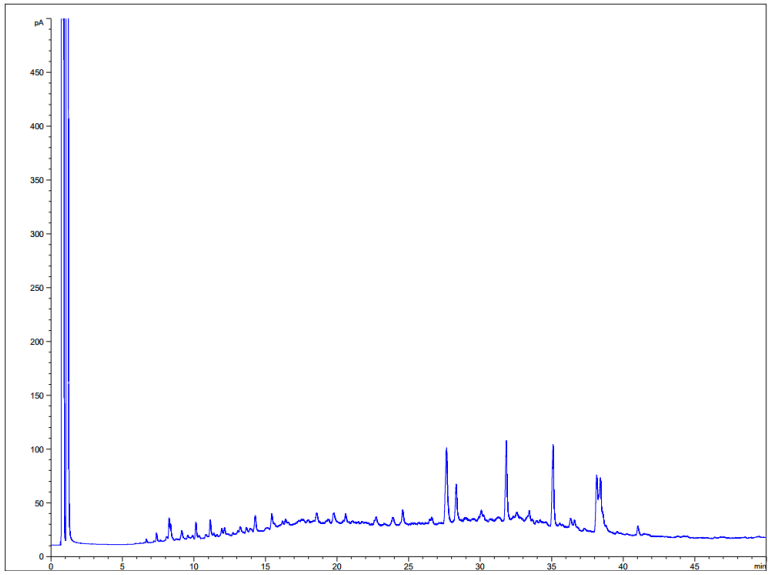

Fig. A2-1. Original sediment sample without urea adduction.

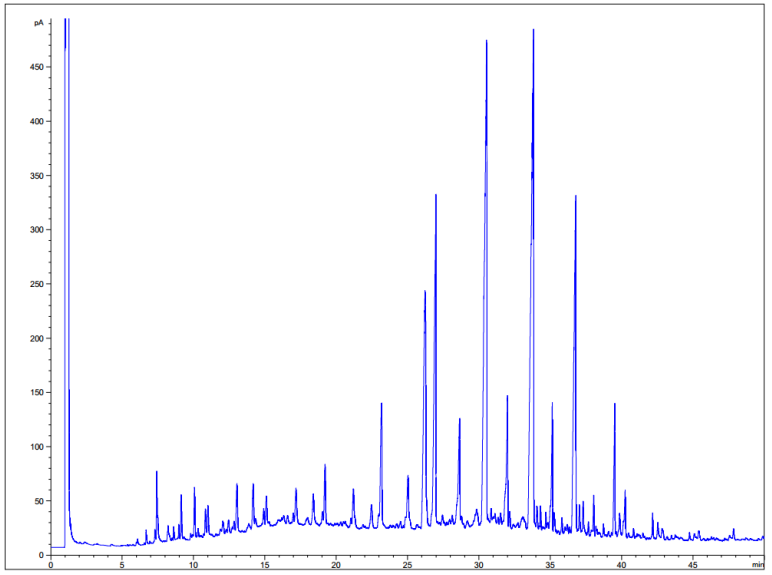

Fig. A2-2. Sediment sample after 1 urea adduction.

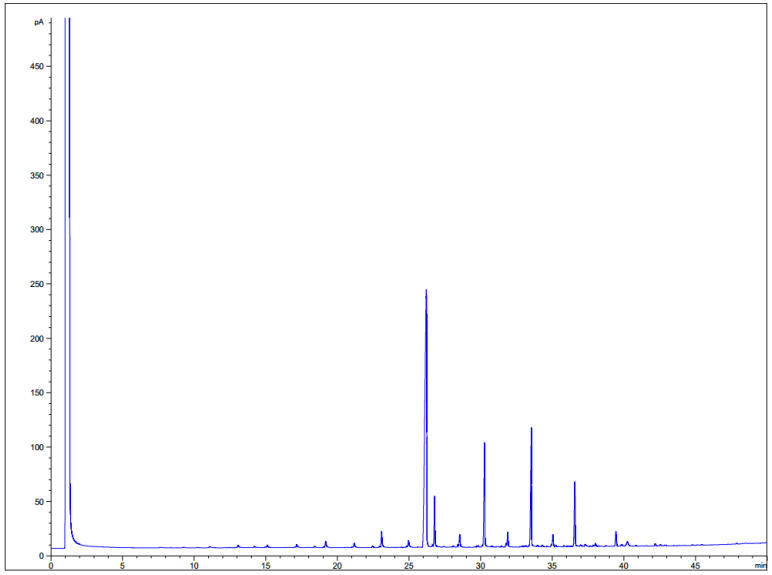

Fig. A2-3. Sediment sample after 2 urea adductions.

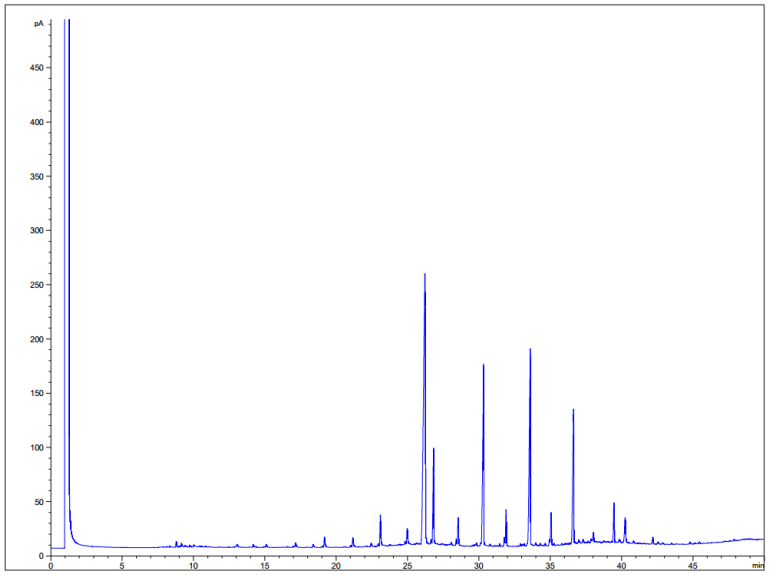

Fig. A2-4. Sediment sample after 3 urea adductions.

A3. Correlation ACL and ACL odd

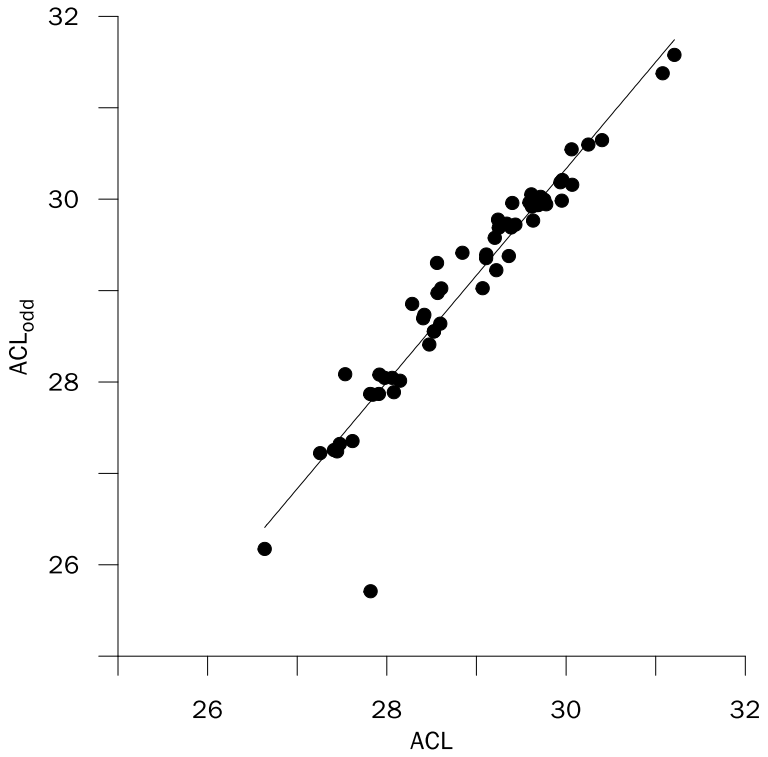

Fig. A3. Correlation between ACL calculated using only odd n-alkane chain length and odd and even chain length n-alkanes. Solid line is linear regression line